

Long Island University

Digital Commons @ LIU

Selected Full-Text Dissertations 2020-

LIU Brooklyn

2023

Calcium involvement in the mechanism of action of Limonene as a penetration enhancer for topical/transdermal drug products

Rucha Suresh Pathak
Long Island University

Follow this and additional works at: https://digitalcommons.liu.edu/brooklyn_fulltext_dis



Part of the [Pharmacy and Pharmaceutical Sciences Commons](#)

Recommended Citation

Pathak, Rucha Suresh, "Calcium involvement in the mechanism of action of Limonene as a penetration enhancer for topical/transdermal drug products" (2023). *Selected Full-Text Dissertations 2020-*. 11.
https://digitalcommons.liu.edu/brooklyn_fulltext_dis/11

This Dissertation is brought to you for free and open access by the LIU Brooklyn at Digital Commons @ LIU. It has been accepted for inclusion in Selected Full-Text Dissertations 2020- by an authorized administrator of Digital Commons @ LIU. For more information, please contact natalia.tomlin@liu.edu.

**CALCIUM INVOLVEMENT IN THE MECHANISM OF ACTION OF LIMONENE
AS A PENETRATION ENHANCER FOR TOPICAL/TRANSDERMAL DRUG
PRODUCTS**

**A DISSERTATION SUBMITTED
IN PARTIAL FULFILLMENT OF THE REQUIREMENTS
FOR THE DEGREE OF
DOCTOR OF PHILOSOPHY**

**WITH SPECIALIZATION IN PHARMACEUTICS
TO THE FACULTY OF THE ARNOLD & MARIE SCHWARTZ COLLEGE
OF PHARMACY AND HEALTH SCIENCES
LONG ISLAND UNIVERSITY
BROOKLYN, NEW YORK**

MAY 2023

BY

Rucha Suresh Pathak

Division of Pharmaceutical Sciences

Approval by: Sponsoring Committee

_____,
Dr. Grazia Stagni – Chair

Dr. Kenza Benzeroual (Committee Member)

Dr. Rutesh Dave (Committee Member)

Dr. Amit Joshi (Committee Member)

Dr. David Taft, Division Chair

Joseph J. Bova,
Vice Dean of Academic Affairs

I. ACKNOWLEDGEMENTS

This project would not have been possible without the support of many people. Words cannot express my gratitude to my professor and chair of my committee, Dr. Grazia Stagni for her invaluable patience, feedback, support, and tutelage during the course of my PhD degree. I would also like to express my deepest appreciation to my defense committee, Dr. Kenza Benzeroual, Dr. Rutesh Dave, and Dr. Amit Joshi for their valuable time and cooperation. I am grateful for their advice and constructive criticism which led to the successful completion of the thesis.

My gratitude extends to the Department of Pharmaceutical Sciences for the funding opportunity to undertake my coursework at the Long Island University and for giving me the opportunity to learn and thrive in this Ph.D. journey. Many thanks to all the faculty advisors and the staff at Long Island University for providing the research facility and important guidance on the coursework throughout my PhD degree.

I am also grateful to my lab mates, friends, and cohort members, for their help during experiment set-ups, late-night experiment sessions, troubleshooting problems and moral support. I would like to extend a special thanks to Cora Kaiser for the animal handling training.

Lastly, I would like to extend my gratitude to my family, especially my parents, my sister, and numerous friends who endured this long process with me, always offering support and love. I want to thank them for always being there for me, making me

smile, listening to me, advising me, believing in me during the ups and downs, I am lucky to have them by my side.

Another round of appreciation for everyone in my life who I have come across and who have helped me because I wouldn't be who I am without them. I thank all those who directly and indirectly helped me in successful completion of this work.

II. ABSTRACT

The addition of chemical permeation enhancers (CPE) to a topical dermatological formulation is the prevalent approach to improve permeability of active pharmaceutical ingredients (API) across the stratum corneum. Terpenes have been used as CPEs for a long time since they are safe and non-irritating. Limonene is one such terpene majorly found in essential oils extracted from citrus fruits and many varieties of cannabis. Studies performed using Limonene as PE show that Limonene was able to increase the flux of the drug by many folds. Limonene acts as an agonist to transient receptor potential ankyrin 1 (TRPA1) receptor – the activity of which is highly Ca^{2+} dependent. Since, calcium is found in the entire epidermis, the purpose of this study was to evaluate whether the above-mentioned properties of Limonene are related to its penetration enhancing effects. The aim of this study was to investigate whether the permeation enhancers R-Limonene (R-L) & S-Limonene (S-L) might act by decreasing the extracellular Ca^{2+} concentration that it is responsible for the tight cell-cell adhesion in the stratum corneum.

The first step was to find the optimal concentration of limonene that enhances the penetration of a model drug, diphenhydramine (DPH) from topical dermatological gels. Seven gels containing 5% DPH were prepared with 0 (control) and three increasing concentrations of R-L or S-L (1.00, 1.75, and 2.50 %) using simple dispersion method. An *in-vitro* release study across regenerated cellulose membrane using Franz cell apparatus was conducted to evaluate any possible physical

interaction by assessing release parameters like flux and cumulative amount permeated. Then, an ex vivo study using porcine ear skin was performed to select the optimal percentage of R-L and S-L. The 1.00% R-L and 1.00% S-L increased permeability of DPH by 82.37% and 111.51%, respectively compared to control formulation, whereas higher percentages were not significantly different from control gel. Then, the calcium channel blocker diltiazem (DTZ) was added to the selected formulations to evaluate whether it counteracts the penetration enhancing effects of R-L or S-L. These formulations were tested again in-vitro on regenerated cellulose membrane to evaluate physical interaction before proceeding to the in vivo studies. All gels were tested for consistency, transparency, and uniformity of content. Samples were analyzed with a bioanalytical method specifically developed and validated for DPH/DTZ combination.

This was followed by testing the suitability of microdialysis technique for DPH and DTZ through recovery and retrodialysis (loss) experiments. Finally, in vivo experiments were performed on a rabbit model. A randomized, crossover, single-dose, four treatment study design was chosen so that each rabbit would receive the test and reference formulation. The four gel combinations – control (5% DPH); test (5% DPH + 1%R-L or 1% S-L); control + DTZ (5% DPH + DTZ); test + DTZ (5% DPH + 1% R-L or 5% DTZ) were applied to the rabbit's dorsal surface on the same day and dermal concentration profiles of DPH were assessed using microdialysis. The pharmacokinetic parameters such as C_{max} and AUC_{inf} were estimated using Phoenix WinNonlin Non Compartmental Analysis and studied for comparison between

different formulations. The gels containing R-L or S-L showed slightly higher dermal exposure of DPH compared to the control gel. Whereas the dermal exposure from the gel containing DTZ was not different from the control gel. The results support the hypothesis that Limonene inhibition of Ca^{+2} activity in the skin might contribute to its penetration enhancing effect, although more in-vivo experiments are necessary to further prove this hypothesis.

III. Table of Contents:

1. Background.....	18
2. Hypothesis	23
3. Objective and Specific Aims	26
4. Study Design.....	29
5. Introduction	34
5.1 Skin Structure	34
5.2 Topical Dermatological Delivery System (TDDS)	36
5.2.1 Introduction and Classification	36
5.2.2 Topical Drug Classification System (TCS)	37
5.2.3 Percutaneous Penetration	38
5.3 Chemical Structures of Moieties	45
5.4 Gel Formulation	45
5.5 Microdialysis (MD).....	45
6. Preliminary Experiments	49
6.1 Bioanalytical method validation.....	49
6.1.1 Purpose.....	49
6.1.2 Method	50
6.1.3 Stability Studies	54
6.1.4 Results and Discussion	55
7. Gel Preparation and Quantitation	65
7.1 Method of gel preparation	65

7.2	Method for gel quantitation: Drug Content Assay	66
7.3	Results and Discussion.....	67
8.	<i>In vitro</i> Release Studies	69
8.1	Purpose	69
8.2	Method	71
8.3	Result and discussion	72
9.	In Vitro Permeation Studies	75
9.1	Purpose	75
9.2	Method	75
9.3	Result and discussion	76
10.	In vitro microdialysis.....	81
10.1	Purpose	81
10.2	Method.....	82
10.2.1	In-house probe manufacturing procedure	82
10.2.2	In vitro Microdialysis & Retrodialysis Method	83
10.3	Results and discussions	85
11.	In vivo experiments:	88
11.1	Purpose	88
11.2	Method (dMD Study Design).....	89
11.3	Results and Discussion	92
12.	Conclusion and Summary.....	102
13.	References	104

IV. List of Figures:

Figure 1: Schematic representation of limonene induced permeation enhancement (modified from [11])	24
<i>Figure 2: Study design of DPH and two enantiomers of Limonene and a Calcium channel blocker</i>	29
Figure 3: Study design to detect possible physical-chemical interaction between the drug and calcium channel blocker on the drug release rate.	30
Figure 4: Example of in vivo study design showing position of microdialysis probes and gel application areas.	32
Figure 5: Pictorial Illustration of the Physiology of the skin [15]	34
Figure 6: Classification of Topical Drug Products Based on Qualitative & Quantitative Composition [21]	37
Figure 7: Mechanism of drug penetration through skin from a topical formulation (Modification from [18]).....	39
Figure 8: Various penetration pathways through the skin [30].....	40
Figure 9: Microdialysis technique illustrations showing linear probe with semipermeable membrane. [48].....	46
Figure 10: Representative Chromatogram from Agilent 1100 HPLC with DAD detector at $210 \pm 4\text{nm}$ with a reference band at $360 - 100\text{nm}$. Chromatogram for a blank sample: Lactate Ringer Solution	58

Figure 11: Representative Chromatogram from Agilent 1100 HPLC with DAD detector at $210 \pm 4\text{nm}$ with a reference band at $360 - 100\text{nm}$. Chromatogram for a DPH & DTZ in LRS at peak retention time of 6.5min and 7.4min, respectively.....	58
Figure 12: Franz diffusion cell apparatus with donor and receptor chamber	71
Figure 13: Franz Cell Assembly [50].....	71
Figure 14: The release rate profiles of DPH for Franz cell diffusion study using cellulose membrane is showed here. Graphical representation of cumulative amount of drug (DPH) released from all seven formulations using cellulose membrane. Each line represents an average of three replicates. The error bars show the standard deviation of the three replicates.	73
Figure 15: Time course of cumulative amount of drug (DPH) released from all seven formulations using porcine ear skin is showed here. Each line represents an average of three replicates. The error bars show the standard deviation of the three replicates.	77
Figure 16: Time course of cumulative amount of drug (DPH) released from all six formulations (three formulations without CCB and three containing CCB) using porcine ear skin is showed here. Each line represents an average of three replicates. The error bars show the standard deviation of the three replicates.....	78
Figure 17: In vitro assembly set up shows the probe spacing in the jacketed cylinder.	84
Figure 18: In vitro assembly set up: Shows the entire assembly set up for Gain and Loss experiments.	84

<i>Figure 19: Linear relationship of Steady State Recovery of DPH from bulk in vitro at three different concentrations (1, 5 and 10 µg/mL). (Mean ± SD, n=3).....</i>	<i>85</i>
Figure 20: Schematic representation of Rabbit model for In vivo MD study design showing position of microdialysis probes and gel application areas.....	90
Figure 21: Probe application gel patch area with a diameter of 2.5 cm.....	91
Figure 22: In vivo experimental set-up showing gel application areas on the shaved rabbit dorsum	91
Figure 23: Concentration-time profiles of DPH in dermis after topical administration of four gel formulations (DPH + DTZ(CD), DPH (C), DPH + 1% R-L (R1), DPH + DTZ + 1% R-L (R1D)) on shaved dorsal skin of three rabbits. Vertical bars represent standard deviation of six probes from three rabbit studies.	92
Figure 24: Average dermal Concentration-time profiles of DPH after topical administration of four gel formulations (DPH + DTZ(CD), DPH (C), DPH + 1% R-L (R1), DPH + DTZ + 1% R-L (R1D)) on shaved dorsal skin of three rabbits: (A) – Rabbit 1, (B) – Rabbit 2, (C) – Rabbit 3. Vertical bars represent standard deviation of two probes within the same rabbit.	93
Figure 25: Maximum dermal concentration of DPH in the three rabbits from all gel formulations. C: Control DPH, CD: Control DPH + DTZ, R1: DPH + 1% R-L, R1D: DPH + 1% R-L + DTZ.	94
Figure 26: Total dermis exposure of DPH in all three rabbits from all four gel formulations C: Control DPH, CD: Control DPH + DTZ, R1: DPH + 1% R-L, R1D: DPH + 1% R-L + DTZ.	95

Figure 27: Concentration-time profiles of DPH in dermis after topical administration of four gel formulations (DPH + DTZ, DPH, DPH + 1% S-L (S1), DPH + DTZ + 1% S-L (S1D)) on shaved dorsal skin of three rabbits.....	96
Figure 28: Average dermal Concentration-time profiles of DPH after topical administration of four gel formulations (DPH + DTZ(CD), DPH (C), DPH + 1% S-L (S1), DPH + DTZ + 1% S-L (S1D)) on shaved dorsal skin of three rabbits: (A) – Rabbit 1, (B) – Rabbit 2, (C) – Rabbit 3. Vertical bars represent standard deviation of two probes within the same rabbit.	97
Figure 29: Maximum dermal concentration of DPH in all three rabbits from all gel formulations C: Control DPH, CD: Control DPH + DTZ, S1: DPH + 1% S-L, S1D: DPH + 1% S-L + DTZ.....	98
Figure 30: Total dermis concentration of DPH across time in all three rabbits from all four gel formulations C: Control DPH, CD: Control DPH + DTZ, S1: DPH + 1% S-L, S1D: DPH + 1% S-L + DTZ.....	98
Figure 31: TEWL vs AUC for all six rabbit studies.	99

V. List of Tables

Table 1: Chemical Penetration enhancers [36]	42
Table 2: Chemical structure of important moieties used in the gel formulations. [43] [44].....	45
Table 3: Quality Control concentrations of DPH used to verify sample analysis	54
Table 4: Quality Control concentrations of DTZ used to verify sample analysis.	54
Table 5: Inter-day HPLC method validation of DPH and DTZ in LRS (n=6)	56
Table 6: Intra-day HPLC method validation of DPH and DTZ in LRS (n=6)	57
Table 7 – Summary of HPLC Method validation.....	61
Table 8: Back calculated concentrations for DPH & DTZ.....	62
Table 9: ANOVA single factor analysis for DPH (10 µg/ml) single vs. combination	63
Table 10: Formulation chart representing quantity of each ingredient in %w/w for all DPH gels prepared in-house.	65
Table 11: Results of quantitation of each gel formulation.....	67
Table 12: Flux and cumulative amount of DPH permeated from three replicates of in vitro release study using cellulose membrane. (mean ± SD, N=6).....	73
Table 13: Flux (J), cumulative amount permeated after 6h and permeability coefficient (Kp) values from three replicates of in vitro permeation studies using porcine ear skin. (mean ± SD, N=6)	77
Table 14: Flux (J), cumulative amount of DPH permeated after 6h and permeability coefficient (Kp) values from three replicates of in vitro permeation studies using	

porcine ear skin for formulations with and without 1% R-L and S-L. (mean \pm SD, N=6)	79
Table 15: Results of in vitro % gain experiments for DPH and DTZ (mean \pm SD, N = 3)	86
Table 16: Result of in vitro % loss experiments for DPH and DTZ (mean \pm SD, N = 3)	86
Table 17: In vivo comparison of the primary endpoint for test and reference DPH gels	99
Table 18: Grouping Information Using the Tukey Method and 95% Confidence (N=6).....	100

VI. List of Abbreviations

CPE	Chemical Penetration Enhancer
TRP	Transient receptor potential
TRPA	Transient receptor potential Ankyrin
TRPM	Transient Receptor Potential Melastatin
TRPV	Transient Receptor Potential Vanilloid
CCB	Calcium channel blocker
DPH	Diphenhydramine
DTZ	Diltiazem
R-L/ S-L	R-Limonene/ S-Limonene
SC	Stratum corneum
TDDS	Topical drug delivery system
TDDP	Topical dermatological drug products
TCS	Topical Drug Classification System
DSC	Differential Scanning Calorimetry
FDA	Food and Drug Administration
IACUC	Institution Animal Care and Use Committee
LLOQ	Lower limit of quantification
LOD	Limit of detection
MD/ dMD	Microdialysis/ dermal Microdialysis
AUC	Area under curve
C _{max}	Maximum concentration

ECF	Extra cellular fluid
QC	Quality Control
LRS	Lactated Ringer Solution
BE	Bioequivalence

CHAPTER 1: BACKGROUND

1. Background

The largest organ of the human body is skin which is also one of the preferred routes of drug delivery for both local and systemic targets. The outer layer of the skin, the stratum corneum (SC), functions as a protective barrier layer to the entire body; however, it is also the greatest challenge to delivery of molecules through the skin. Among the several measures available to enhance the penetration of drugs through the skin, the addition of chemical penetration enhancers (CPE) is the most prevalent [1]. Terpenes have been used in topical drug delivery system as CPEs for a long time since they are safe and non-irritating. Limonene is one such terpene majorly found in essential oils extracted from citrus fruits, especially in orange and lemon as well as in many varieties of cannabis [2]. Studies performed using Limonene as CPE show that Limonene was able to increase the flux of the drug by many folds [3]. The application of Limonene as CPE has expanded significantly, however, its mechanism of action has still been elusive.

Terpenes are known to enhance penetration by one of the subsequent methods: by distorting the intercellular lipid matrix, the intracellular keratinocytes or by acting as a solvent for the permeant thereby increasing drug partitioning into the tissue. William and Barry predicted that terpenes might alter the metabolic activity within the skin or exert an influence on the thermodynamic activity/solubility of the drug in its vehicle [4].

Lan et al. studied the effect of terpene CPE on membrane fluidity and membrane potential using HaCaT keratinocytes. HaCaT is a cell line from adult human skin used as a model in number of studies of human skin function. They also studied the potential mechanisms of those terpene compounds used as natural transdermal penetration enhancers. Six terpene compounds, namely menthol, limonene, 1,8-cineole, menthone, terpinen-4-ol and pulegone, were chosen due to their good penetration-enhancement activities. The change of membrane fluidity of HaCaT cells was measured using fluorescence recovery after photobleaching (FRAP) technique. The alteration of membrane fluidity of HaCaT cells was studied using a flow cytometer and the effect of terpene compounds on intracellular Ca^{2+} was investigated. Those terpene compounds significantly enhanced HaCaT cells membrane fluidity and reduced HaCaT cells membrane potentials. Ca^{2+} ATPase activity and intracellular Ca^{2+} of HaCaT cells decreased measurably after being treated with various terpene compounds. Terpene penetration enhancers perhaps changed the membrane fluidity and potentials of HaCaT cells by altering the Ca^{2+} balance of the cell inside and outside, leading to a rise in an increase in the drug transdermal absorption [5].

Kaimato et. al. studied the action of limonene on TRP channels. They investigated the effects of limonene on sensory neurons and heterologously expressed channels in wild-type, TRPV1 and TRPA1 gene-deficient mice in vitro. Limonene increased the intracellular Ca^{2+} concentration in wild-type mouse sensory neurons, which was inhibited by selective inhibitors of TRPA1 whereas limonene failed to stimulate sensory neurons from the TRPA1 (-/-) mouse [6].

Bandell et al. proved that pungent natural compounds present in cinnamon oil, clove oil, mustard oil and ginger all activated TRPA1. Mustard oil induced Ca^{2+} influx in wild type mice, whereas no Ca^{2+} influx was observed in TRPA1 deficient mouse [7]. These studies indicate the indirect connection between limonene and Ca^{2+} concentration, which may lead to the decreased cell-cell cohesion and in turn increased penetration of the API applied topically.

TRPA1 channels respond to an array of irritants with diverse origins and chemical structures. Currently, the mechanism of interaction of mustard oil and other activators with TRPA1 is unknown. Various mechanisms of channel activation are discussed below. First, binding of chemical irritants to TRPA1 may happen through “classical” ligand-receptor interaction. Some receptors bind multiple ligands with diverse structures while most are highly specific. TRPA1 may bind to a large variety of irritant molecules to induce sensory neural excitation. Second, chemically reactive irritants such as mustard oil could form permanent or transient covalent bonds with TRPA1, thereby activating the channel. Isothiocyanates, allicin, and unsaturated aldehydes are reactive compounds capable of forming covalent bonds with cysteine and other residues in proteins. Third, chemically reactive irritants could activate the channel by interfering with signaling pathways that regulate TRPA1. These pathways could include phosphorylation cascades, or regulation of intracellular Ca^{2+} that is known to affect TRPA1 function [8] [9].

Karashima et al. found that terpenes like menthol have bimodal action on TRPA1 channel where it activated the channels at low micromolar concentrations but caused reversible channel blocking at higher concentration [10]. Similar bimodal action of Limonene on TRPA1 was found by Kaimato et al. They found that topically applied limonene stimulates TRPA1 while systemic application of limonene showed inhibitory effects on TRPA1 channel [6].

Menthol is one of the most used terpenes as a CPE. Previous studies to determine the mechanism of action of menthol as CPE have shown it to interfere with calcium channels in the skin by activating TRPM8 channel in the keratinocytes and affect cell-cell cohesion by disturbing extracellular Ca^{2+} concentration [11].

The main purpose of this study is to investigate the possibility that the interference of limonene with calcium channels also contributes to the mechanism of penetration enhancing effects of limonene. This study will raise awareness of possible interactions that may occur when topical and/or transdermal formulations containing Limonene (as a penetration enhancer) are administered to patients taking calcium channel blocker.

CHAPTER 2: HYPOTHESIS

2. Hypothesis

There is massive evidence that Limonene's interference with TRPA1 channels may contribute to the mechanism of limonene-induced penetration enhancing effects in the skin. However, to the best of our knowledge, this interaction has never been proven. The hypothesis of this research project is to investigate whether the permeation enhancers R-Limonene (R-L) & S-Limonene (S-L) might act by decreasing the extracellular Ca^{2+} concentration that is responsible for the tight cell-cell adhesion in the stratum corneum (Figure 1). The first step in this project was to find the optimal concentration of limonene that enhances the penetration of a model drug, diphenhydramine (DPH) from topical dermatological gels. Then, the calcium channel blocker diltiazem (DTZ) was added to the formulations with the best permeation profiles (*ex-vivo*) to evaluate whether it counteracts the penetration enhancing effects of limonene. The two formulations of each R-L and S-L with and without the CCB was then tested *in vivo* along with the two control formulations to evaluate the permeation effects of limonene.

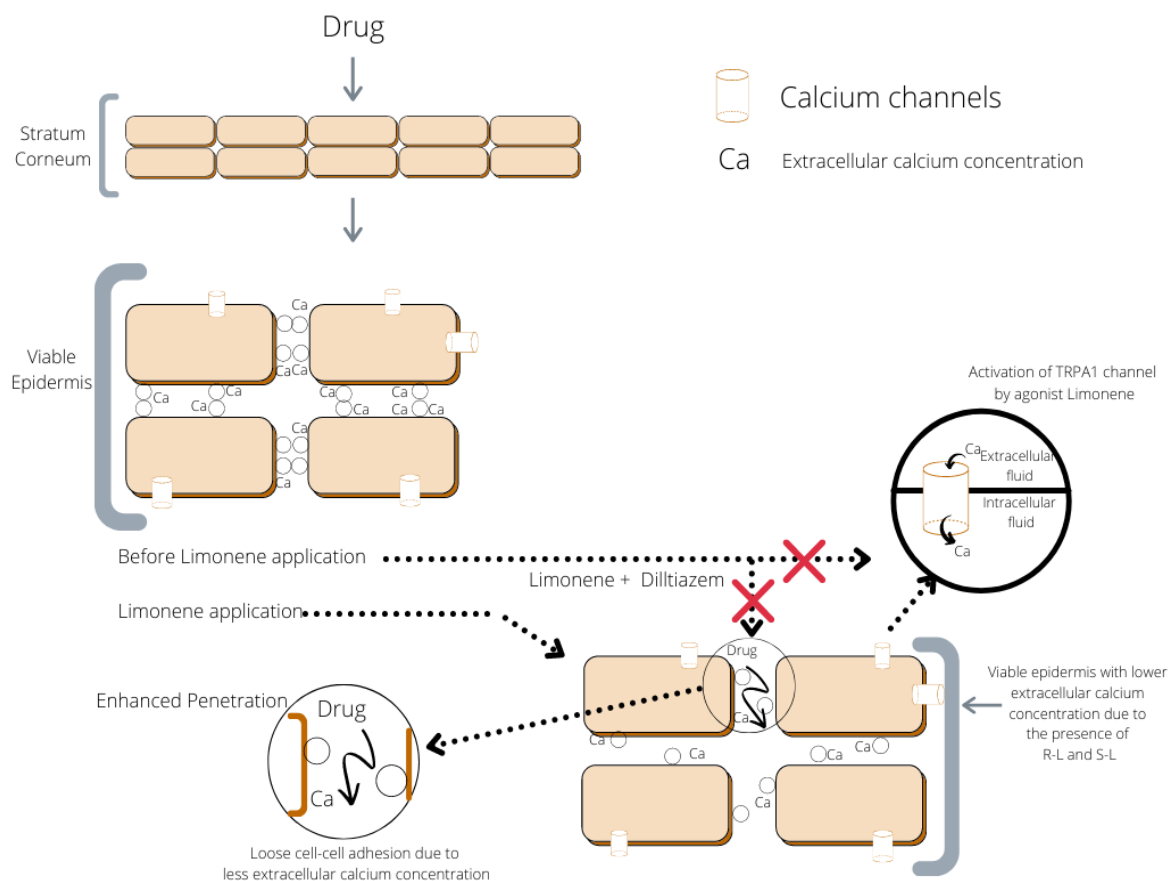


Figure 1: Schematic representation of limonene induced permeation enhancement (modified from [11])

CHAPTER 3: OBJECTIVES & SPECIFIC AIMS

3. Objective and Specific Aims

Overall objective: To investigate whether the mechanism of limonene skin permeation enhancing effect involve interaction with TRP calcium channels.

Groundwork:

- Development and validation of bioanalytical methods for simultaneous determination of diphenhydramine (DPH) and a calcium channel blocker – diltiazem (DTZ).
- To prepare the microdialysis probes in house and perform in vitro microdialysis study (%gain and %loss) to evaluate the suitability of microdialysis technique for the chosen drug: DPH.

Specific Aim 1: To develop and characterize gel formulations containing active drug DPH, CPEs R-L and S-L separately and CCB DTZ, respectively.

Specific Aim 2: To perform *In vitro* Franz cell diffusion studies using cellulose membrane to assess the physical interactions among DPH, DTZ and CPEs R-L and S-L.

Specific Aim 3: To find the optimal concentration of R-L and S-L that enhances the penetration of a model drug, DPH from topical dermatological gels by performing *In vitro* Franz cell diffusion to examine the permeation across porcine ear skin from all six formulations of DPH with three different concentrations of R-L and S-L respectively.

Specific Aim 4: To investigate if DTZ inhibits the permeability of DPH *ex vivo* by performing *In vitro* Franz cell diffusion studies across the porcine ear skin for the formulations containing CCB DTZ.

Specific Aim 5: To perform *In vivo* experiments to assess skin profiles of DPH from various gel formulations using dermal microdialysis technique.

CHAPTER 4: STUDY DESIGN

4. Study Design

The experiments were conducted on dermatological gels prepared in our laboratory. Seven gels containing 5% DPH are prepared with 0 (control) and three increasing concentrations of R-L or S-L (1.00, 1.75, and 2.50 %) using simple dispersion method. All gel formulations are tested for consistency, transparency, and uniformity of drug content with a bioanalytical method specifically developed and validated for DPH/DTZ combination.

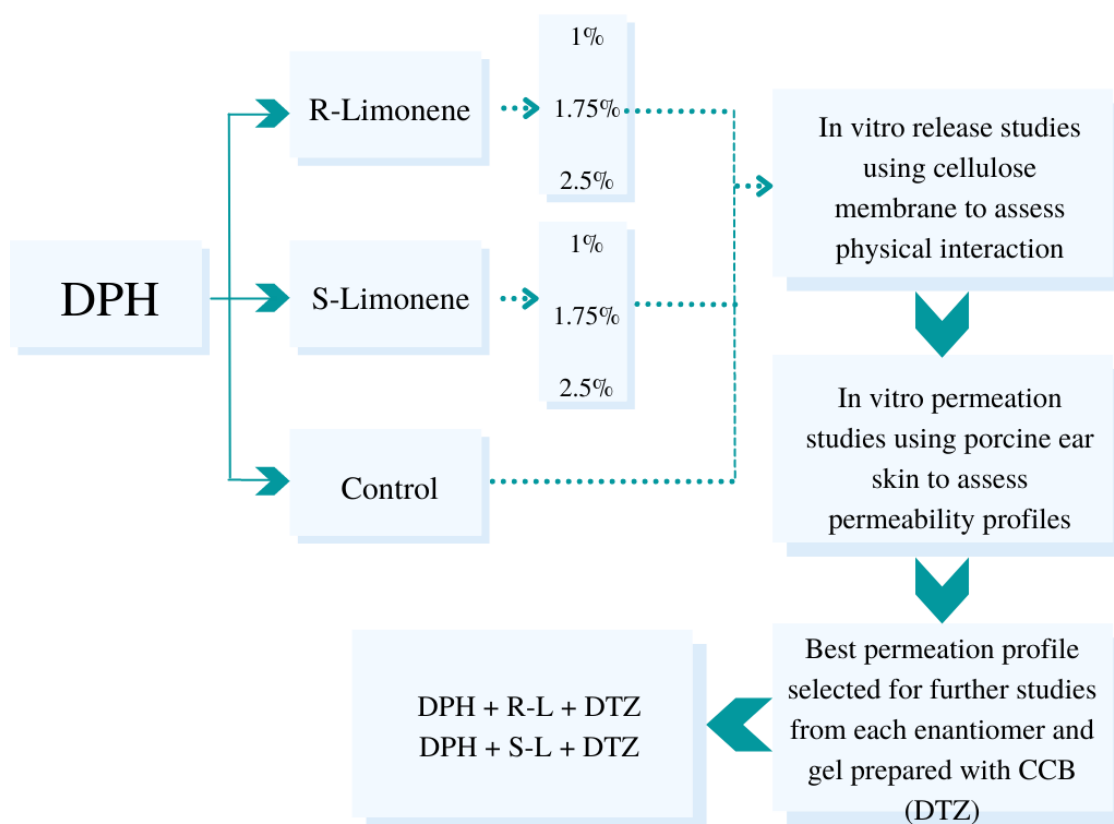


Figure 2: Study design of DPH and two enantiomers of Limonene and a Calcium channel blocker

In-vitro release study across regenerated cellulose membrane (Figure 2) using Franz cell apparatus was conducted to evaluate any possible physical interaction by assessing release parameters like flux and cumulative amount penetrated. Ex vivo study using freshly excised porcine ear skin was performed using the same apparatus to assess permeability profiles of gel formulations and to select the optimum R-L or S-L concentrations (Figure 2). The two gels with the best permeation profiles were then formulated with 5% of DTZ. These gels were tested in vitro for physical interaction using regenerated cellulose membrane and permeability was assessed using the same Franz cell assembly with Porcine ear skin.

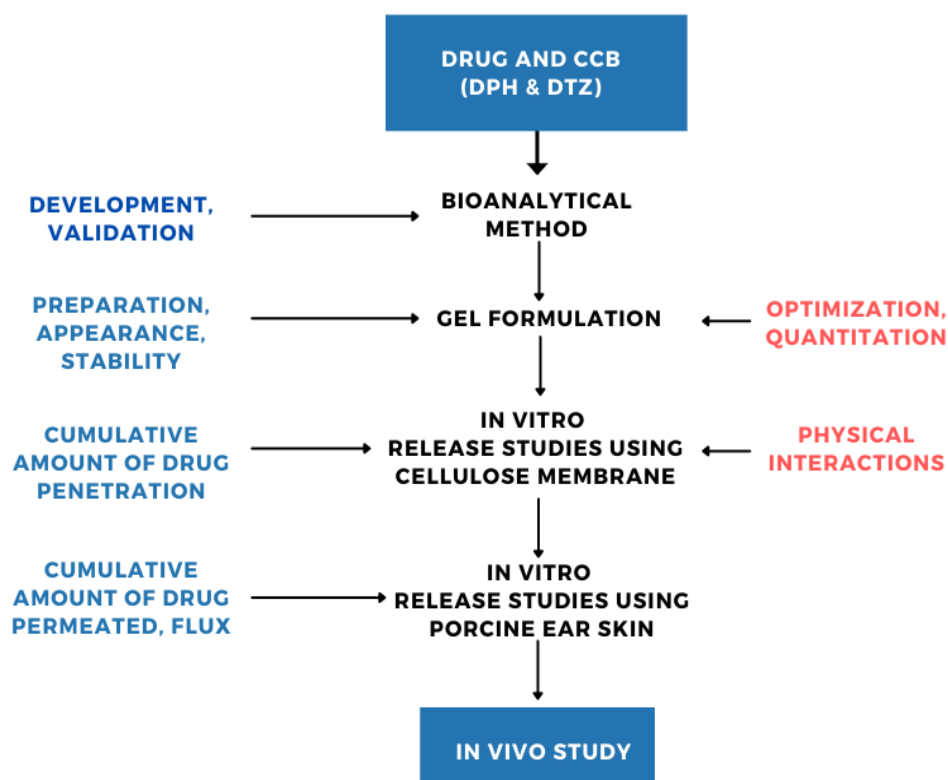


Figure 3: Study design to detect possible physical-chemical interaction between the drug and calcium channel blocker on the drug release rate.

After confirmation of no physical interaction at the *in-vitro* level (Figure 3), the gels were tested *in-vivo* in a rabbit model. A randomized, crossover, single-dose, four treatment study design was chosen such that each rabbit receives the test and reference gel formulation. *In vitro* microdialysis (MD) and retrodialysis experiments were performed prior to *in-vivo* MD to ensure suitability of the technique for the desired drug DPH. During *in vivo* MD, each of the six gels were applied to a 4.906-cm² area to a rabbit's dorsal shaved skin. Four formulations consisting of two controls (i) C (DPH) and ii) CD (DPH + DTZ) and two with the same enantiomer of Limonene (iii) R1 (DPH + R-L) and iv) R1D (DPH + DTZ + R-L) were applied in one microdialysis study at four different sites along with a redistribution probe. Similarly, a second microdialysis study was performed using the two control formulations and the two formulations consisting of S-L. Two microdialysis probes were inserted under the skin before application of each gel formulation. An extra probe was inserted at a different location to evaluate redistribution as illustrated in Figure 4. TEWL at each probe and site was measured prior to gel application.

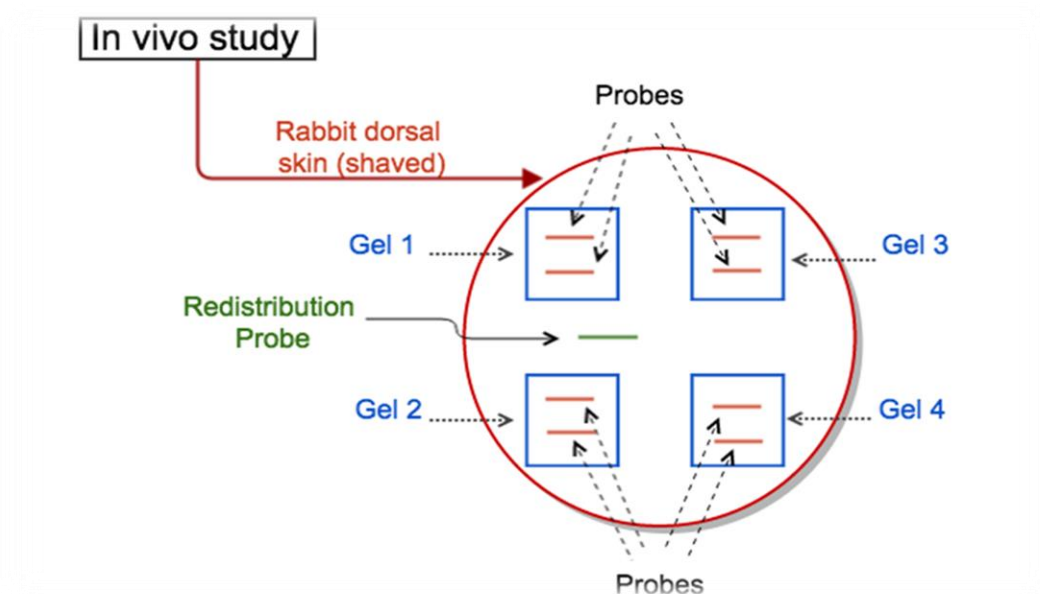


Figure 4: Example of in vivo study design showing position of microdialysis probes and gel application areas.

The microdialysis dialysates were analyzed for drug content using the RP-HPLC method developed for simultaneous estimation of DPH and DTZ. The dermis drug concentration profiles were obtained for each gel and pharmacokinetic parameters such as C_{max} , T_{max} , AUC, etc were estimated using Phoenix WinNonlin Non Compartmental Analysis. These PK parameters along with the average dermis DPH concentration for each gel formulation were evaluated to study the presence of limonene and/or DTZ affecting the dermal pharmacokinetic profile of DPH.

CHAPTER 5: INTRODUCTION

5. Introduction

5.1 Skin Structure

The skin is the largest organ of the human body. It has a surface area of about 2 m² in healthy adults, comprising 16% of the total body mass of an average person [12]. It is a multilayer tissue, and its main function is to guard the body against external circumstances by functioning as an effective barrier to the absorption of exogenous particles [13]. The skin is an important target as well as a main barrier for dermal drug delivery [14].

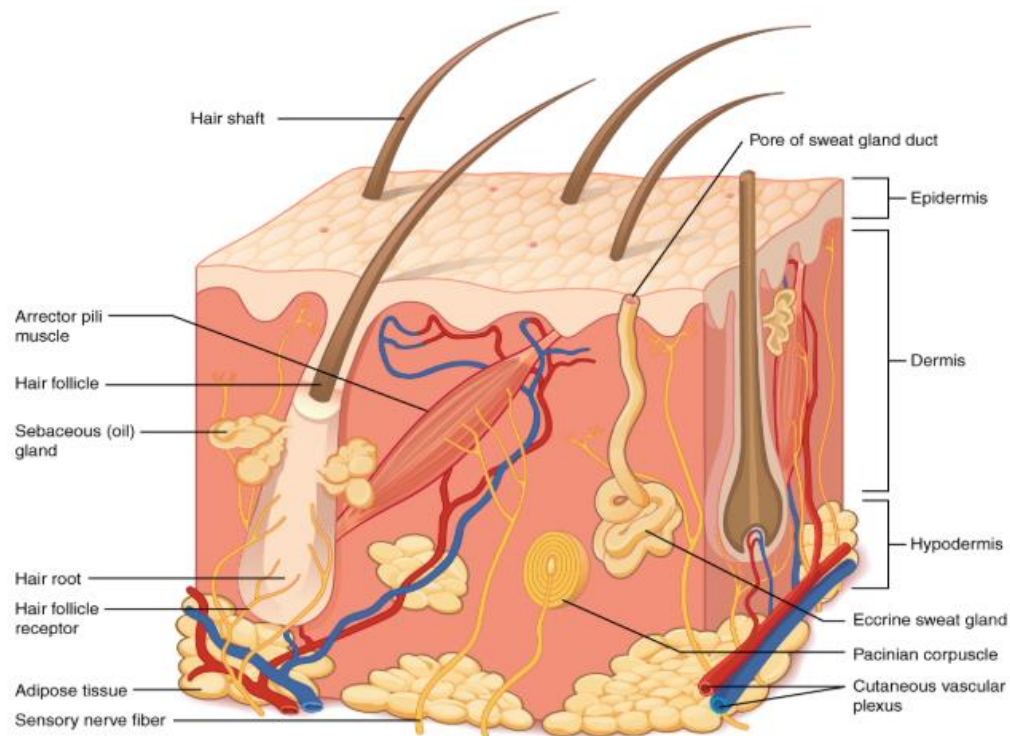


Figure 5: Pictorial Illustration of the Physiology of the skin [15]

The skin consists of three main layers: The epidermis, the dermis, and the subcutaneous tissue (figure 5).

I. Epidermis

The epidermis, excluding the stratum corneum, which is its outside layer, is a viable tissue [13]. There are five sublayers of Epidermis. These are, beginning from the non-viable Stratum corneum, Stratum lucidum (clear layer), Stratum granulosum (granular layer), Stratum spinosum (spinous layer), and Stratum germinativum (basal layer). The epidermis does not have vascularization, and nutrients diffuse from the dermo-epidermal junction to maintain its viability. The cellular content of the epidermis consists mainly of keratinocytes, other cells of the epidermal layer include Melanocytes, Langerhans cells and Merkel cells [16].

II. Dermis

The dermis is thicker than the epidermis and is connected to the epidermis at the level of basement membrane. It comprises of hair follicles, sweat and oil glands, nerve endings, connective tissue, and lymph vessels. The dermis consists of collagen and elastin in its connective tissue which supports the structure of the skin. Two layers of the dermis are Papillary Layer and Reticular Layer.

III. Hypodermis

Subcutis, subcutaneous fat or hypodermis layer are present beneath the dermis. This layer consists of fat cells and numerous blood vessels. This layer keeps the body warm by providing insulation. It is the connecting layer between the skin and underlying tissues of the body, such as muscles and bone [13].

The skin has three main functions: protection, regulation, and sensation [17].

- i. Protection from mechanical impacts and pressure, variations in temperature, micro-organisms, radiation, and chemicals.
- ii. Regulating several aspects of physiology, including body temperature via sweat and hair, and changes in peripheral circulation and fluid balance via sweat.
- iii. Sensation for heat, cold, touch, and pain.

5.2 Topical Dermatological Delivery System (TDDS)

5.2.1 Introduction and Classification

Topical Dermatological Drug Delivery Systems are dosage forms designed to deliver a therapeutically effective amount of drug across a patient's skin locally [18]. Currently, topical delivery has become one of the most promising methods for drug application due to its convenience and ease of application [19]. It also provides a non-invasive alternative to parenteral routes of administration and avoids problems such as needle phobia. It also reduces the load that the oral route commonly places on the digestive tract and liver. It enhances patient compliances and minimizes fluctuation in drug levels [18]. Another advantage of Topical drug delivery systems is that a large area of application is available compared with another route [20].

5.2.2 Topical Drug Classification System (TCS)

Topical dermatological drug products (TDDP) are classified into four classes depending on their qualitative (Q1) and quantitative (Q2) composition as shown in figure 6.

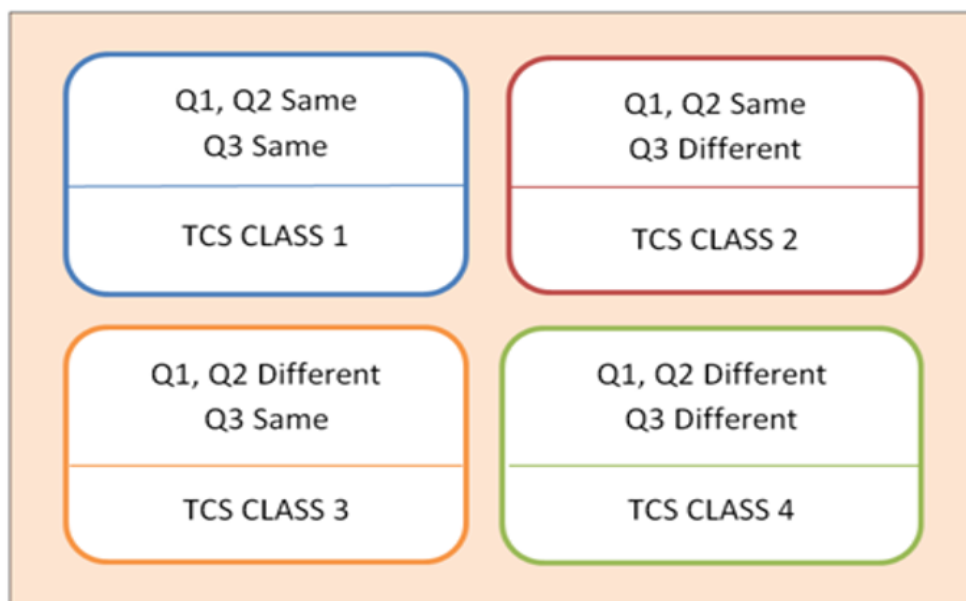


Figure 6: Classification of Topical Drug Products Based on Qualitative & Quantitative Composition [21]

In the figure 6, Q1 and Q2 represent qualitatively and quantitatively same ingredients as the reference listed drug, respectively. Q3 represents the arrangement of matter and microstructure of topical formulations.

TDDP are formulated to show effects on i) Surface and ii) Stratum corneum [22]. Effects on surface include protective action against microbes and moisture, to improve the cosmetic appearance of the skin and the cleansing of germs and dirt.

Majority of TDDP are prepared to produce the following effects on stratum corneum:

1. Protectives that penetrate this layer.
2. Keratolytic action.
3. Moisturizing effect.
4. Viable epidermis and dermis: Anesthetic, anti-inflammatory, antihistamine, antipruritic, etc. are the major classes of drugs that show effect by penetrating this layer.
5. Additional effects: These effects include antimicrobial, emollient, antiperspirant, depilatory [23].

5.2.3 Percutaneous Penetration

5.2.3.1 Stratum Corneum

Before a topically applied drug can produce either local or systemic action, it must penetrate through *stratum corneum*. Percutaneous absorption is defined as penetration of drug substance into various layers of skin and permeation across the skin into systemic circulation (figure 7) [24]. Percutaneous absorption of drug molecules is of particular importance in topical drug delivery system because the drug must be absorbed to an adequate extent and rate to achieve and maintain uniform, therapeutic levels throughout the duration of use. In general, once drug molecule crosses the stratum corneal barrier, passage into deeper dermal layers and systemic uptake occurs

relatively quickly and easily [25]. Stratum corneum mainly consists of the keratinized dead cell called corneocytes [26] that help in the exchange of moisture and oxygen with the external environment. The cells are connected by desmosomes, which maintains the cohesiveness of the layer. The main route of permeation is corneocytes. Hence, larger the size of corneocytes, longer will be the permeation. Other components of the stratum corneum are lipids and water. These lipid molecules join up and form a tough connective network; water acts as a plasticizer preventing cracks and providing flexibility [26].

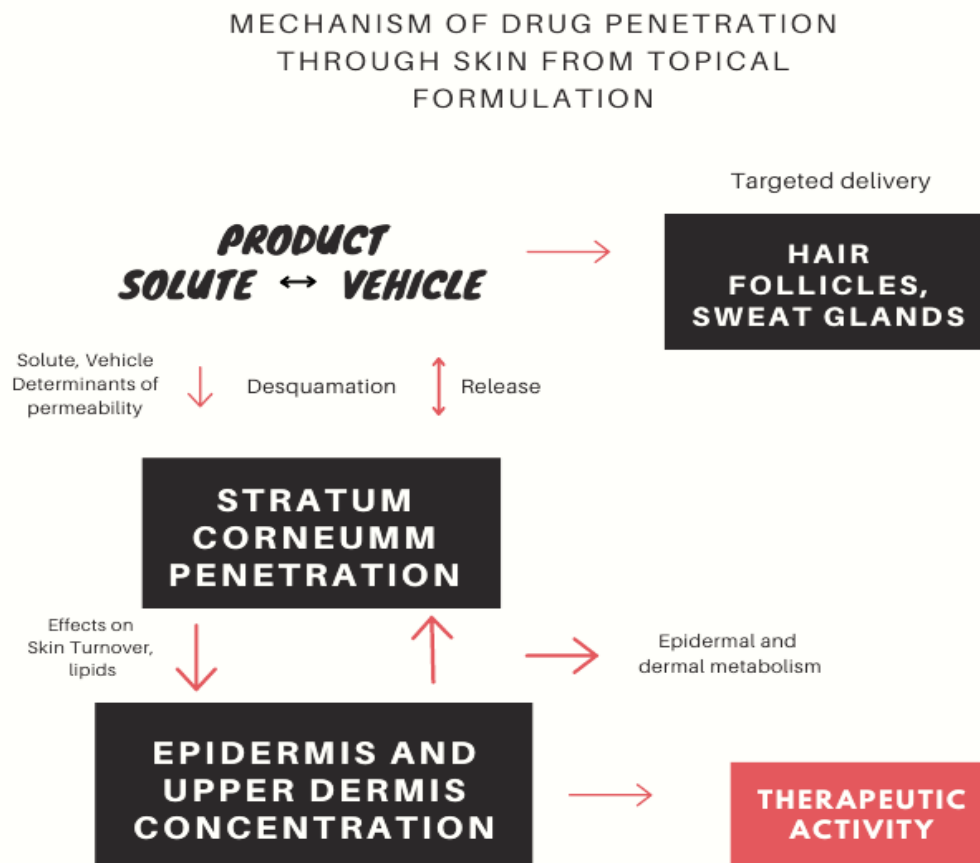


*Figure 7: Mechanism of drug penetration through skin from a topical formulation
(Modification from [18])*

5.2.3.2 Permeation Pathways

There are three different skin penetration pathways by which drugs can cross the SC, namely, the transcellular (through the cells), transappendageal (through hair follicles or sweat glands), and intercellular pathways (between the cells) (figure 8) [27]. The main components of epidermis layer are corneocytes which are composed of highly hydrated keratins. Hence, hydrophilic drugs tend to pass through the transcellular pathway provided by highly hydrated keratins [28]. Likewise, intercellular permeation creates a favorable route for lipophilic drugs, as diffusion of these compounds is guided by the lipid matrix. Modest dermal transport of drugs occurs via the transappendageal pathway, where a mere 0.1% of the total skin surface is covered by hair follicles and sebaceous glands [29].

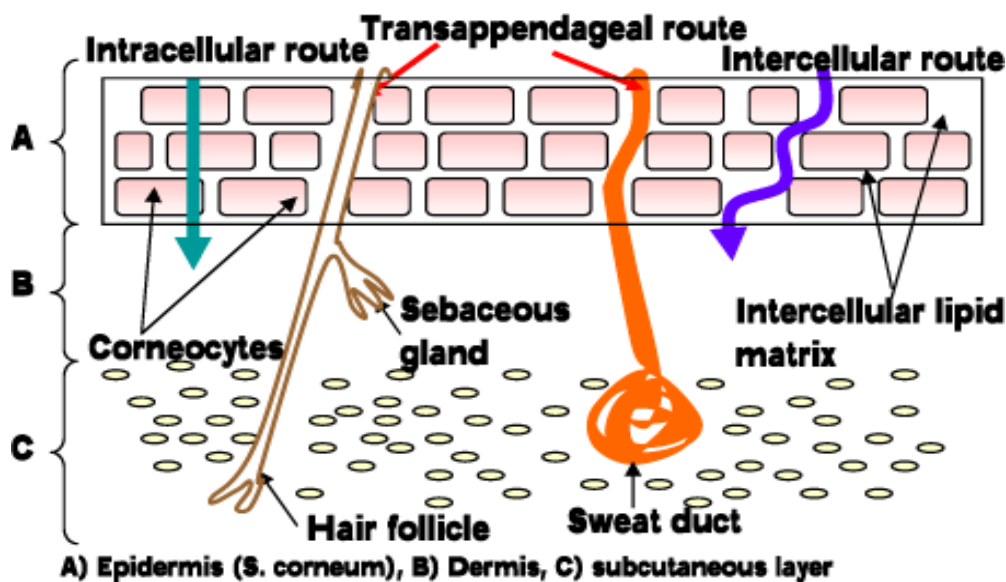


Figure 8: Various penetration pathways through the skin [30]

5.2.3.3 Penetration Enhancers

These are compounds which promote skin permeability by altering the skin as a barrier to the flux of a desired penetrant [31]. There are various reasons penetration enhancers are used. Some of them include: to transfer the delivery of drugs which are ionizable (Example: timolol maleate) and impermeable (Example: heparin); to maintain drug levels in blood, to provide higher dose of less potentially active drugs (Example: Oxymorphone), to deliver high molecular weight hormones and peptides and to lessen the lag time of transdermal drug delivery system [32] [33] [34].

Chemical penetration enhancers (CPEs), or accelerants have several advantages in topical drug delivery. These are painless, noninvasive and have the capacity to increase the transdermal flux in comparison with passive diffusion. Chemical enhancers have been used by several investigators in the past to demonstrate these important properties as well as to better understand the mechanisms of penetration enhancement. It has been postulated that these compounds can enhance topical and/or transdermal drug delivery by perturbing the stratum corneum, increasing partition coefficient or increasing solubility (Table 1) [35].

Table 1: Chemical Penetration enhancers [36]

Chemical enhancers	These include three mechanisms.	1. Pyrrolidones
	1. By disturbing the ordered structure of SC.	2. Azones
	2. By interacting with the proteins (intercellular).	3. Oxizolidinones
	3. By improving drug partition through SC.	4. Cyclodextrines
		5. Sulphoxides and chemicals like dimethyl sulphoxide (DMSO), dimethyl formamide (DMF), dimethyl acetamide (DMAC)
		6. Amides and amines
		7. Fattyacids (capric acid, lauric acid and myristic acid
		8. Surface active agents
		9. Terpenes

5.2.3.4 Terpenes as Penetration Enhancers (PEs) and the source of variability in permeation between enantiomers

Terpenes and terpenoids are essential components of essential oils. They are formed of repeating isoprene (C_5H_8) units and have low irritancy potential [37]. Terpenes are relatively better than other penetration enhancers because they are less toxic, less irritating to the skin and easily available. Terpenes with high lipophilicity, smaller size, lower boiling points, lower vaporization energy and higher degree of unsaturation are good candidates in general with some exceptions.

Cornwell and Barry used twelve sesquiterpene compounds obtained from natural volatile oils as penetration enhancer for 5-Fluorouracil and found 20-fold increase in flux when pretreated with nerolidol. When used along with a polar solvent- ethanol, the flux increased by 13-fold. [38].

Differential Scanning Calorimetry (DSC) showed that when L-Menthol was used as an enhancer, the skin permeation of testosterone increased by forming a eutectic mixture with the menthol. Hence, the initial melting point of testosterone drops from 155°C to 39.9°C. This increases the solubility of the formulation resulting in enhanced absorption. Similar behavior was observed by Phaechamud et al. during DSC analysis of 1:1 menthol/camphor mixture with Ibuprofen. The solubility of Ibuprofen in this mixture increased by four folds [39]. By making the drug more soluble, Menthol tries to alter the barrier function properties of Stratum Corneum. [32].

According to Kaplun et al, in a study performed on rat skin, it was found that Eucalyptus was the most active oil. It increased the permeation of 5-fluorouracil by a factor of 60 in comparison to peppermint oil and turpentine oil which produced a 48-fold and 28-fold increase in enhancement, respectively.

In the experiments of William et al, highest absorption was obtained with mixtures having 80% Propylene Glycol (PG) content and it was found that activity of terpene depended on PG-content. Terpenes increased lipid disruptions in the SC and high PG-content promoted more drug-partitioning thus, increasing the overall permeation.

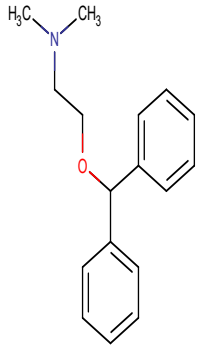
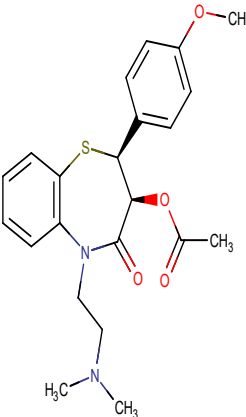
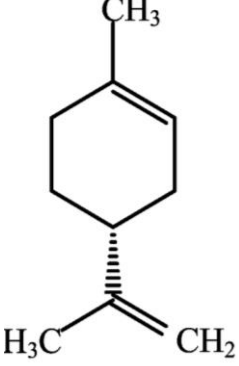
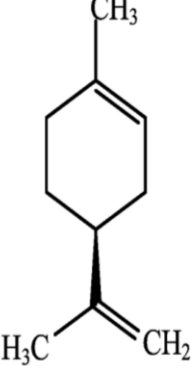
The application of limonene as penetration enhancer has expanded significantly, but its potential effects on cellular metabolism have been elusive. Park et al. found that limonene directly binds to the adenosine A(2A) receptor, which may induce sedative effects. Results from an in vitro radioligand binding assay showed that limonene

exhibits selective affinity to A(2A) receptors. In addition, limonene increased cytosolic cAMP concentration and induced activation of protein kinase A and phosphorylation of cAMP-response element-binding protein in Chinese hamster ovary cells transfected with the human adenosine A(2A) receptor gene. Limonene activated adenosine A(2A) receptors and thereby increased cytosolic calcium concentration [40].

Limonene is a naturally occurring monoterpene, commonly used as permeation enhancer in Topical dermatological formulations. Most naturally occurring chiral compounds are found as a single optical isomer except Limonene; available as R-(+) and S(-) enantiomers. The configuration of the two enantiomers differs at the stereogenic center and hence differ in biological activity and taste [41]. Hence, we should consider that the penetration enhancement effect of terpenes on the SC can be different in different vehicle systems due to the differences in physicochemical properties of these solvents and their interactions with the SC [42]. When terpenes are used along with co-solvents like propylene glycol (PG) or ethanol, they've shown synergistic effects. In addition, other factors including skin type, pH values, and formulation ingredients should also be considered as the sources of experimental variabilities.

5.3 Chemical Structures of Moieties

Table 2: Chemical structure of important moieties used in the gel formulations. [43] [44]

Diphenhydramine	Diltiazem	R-Limonene	S-Limonene
			

5.4 Gel Formulation

A gel is a semisolid preparation consisting of network of cross-linked polymer distended in a liquid medium. The interaction between solid state polymer and the liquid component will determine its properties. Topical gel formulations are less greasy and can be easily removed from the skin and hence are an acceptable delivery system for drugs. In comparison to cream and ointments, gel formulation provides better application property and stability [45].

5.5 Microdialysis (MD)

Microdialysis is a well-established technique for continuous sampling of drugs at the site of action, e.g., sampling the unbound drug concentration in the dermis and subcutaneous tissue [46]. Important advantages of MD over traditional sampling techniques include increased sampling frequency to characterize the concentration-

time profile. In addition, purification is not needed for subsequent analysis, because sampling is done via the semipermeable membrane of a dialysis fiber. Therefore, MD can be used as an evaluation method for studying the disposition of drugs in the skin [47].

The technique of MD has found applications in several therapeutic areas and drug delivery systems i.e., transdermal, neurotransmitters, cytokines, macromolecules like proteins, anti-bacterial, analgesics, and local anesthetics.

Linear Microdialysis

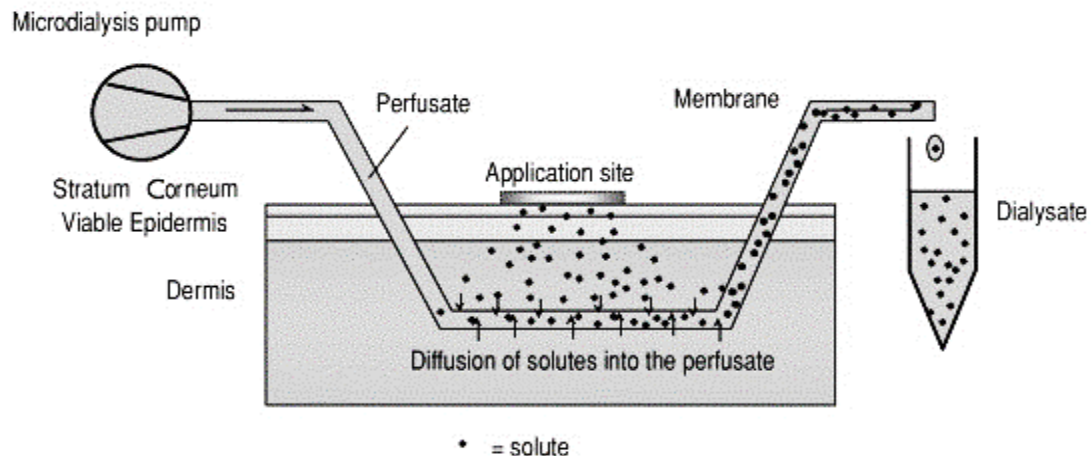


Figure 9: Microdialysis technique illustrations showing linear probe with semipermeable membrane. [48]

In MD, a probe consisting of a hollow dialysis membrane (polyacrylonitrile, molecular weight cutoff 50 kDa) is continuously perfused with an isotonic perfusate and the dialysate is collected at regular intervals of time (Figure 9). Therefore, molecules present in the interstitial fluid cross the dialysis membrane of the MD

probe by passive diffusion. The concentration gradient, diffusion coefficient, and area of diffusion affect the flux through the semipermeable membrane. However, because of the continuous fluid flow inside the probe, equilibration between extracellular fluid (ECF) and the perfusate is incomplete during microdialysis and a correction factor must be used to estimate the actual interstitial fluid.

Before the use of MD *In vivo*, the following must be carefully considered:

- (i) Perform *In vitro* studies to select the optimal membrane material for the intended study,
- (ii) Assess the similarity in composition of perfusate and extracellular fluid, and
- (iii) Measure the adequacy of the quantification method for microdialysis samples that usually contain very low analyte concentrations [11].

CHAPTER 6: PRELIMINARY EXPERIMENTS

6. Preliminary Experiments

6.1 Bioanalytical method validation

6.1.1 Purpose

The availability of selective, sensitive, and validated analytical methods for the quantitative evaluation of drugs and their metabolites is indispensable for successful nonclinical and clinical studies [49]. Any analytical method must be validated to determine its suitability for the planned study. Validation of a bioanalytical methods should include all the procedures that demonstrate that a method used for quantitative measurement of analytes in a given biological matrix is reliable and reproducible for the intended use. The selected analytical method must be validated for: accuracy, precision, specificity, detection limit, quantitation limit, linearity and range. For accuracy and precision, the mean value should be within $\pm 15\%$ of the theoretical value, except at the lower limit of quantification (LLOQ), where it should not exceed $\pm 20\%$. At least six replicates such as intraday (within a day) and inter-day (between days) calibration should be performed to validate above mentioned bio-analytical method parameters.

6.1.2 Method

6.1.2.1 Materials

6.1.2.1.1 Diphenhydramine:

Source	SIGMA LIFE SCIENCES
Lot Number	MKBQ9569V
Catalog Number	D3630-50G
Purity	>98%

6.1.2.1.2 Diltiazem:

Source	SIGMA LIFE SCIENCES
Lot Number	MKBQ9569V
Catalog Number	D3630-50G
Purity	>98%

All other chemicals were HPLC grade.

6.1.2.2 Instrumentation

The HPLC equipment consisted of an Agilent 1100 series (Agilent Technologies, Santa Clara, CA) consisting of degasser (G1379B), binary pump (G1311A), auto-sampler (G1329A), auto-sampler thermostat (G1316A), Column Oven (G1329A), DAD Detector (G1315B). The integration system was Agilent ChemStation (Version 10.02).

6.1.2.3 Assay Method

A reversed phase (RP) HPLC method for simultaneous estimation of diphenhydramine and diltiazem was developed. An ACE equivalent C18 5 μ m 100 x 4.6mm was used at the autosampler temperature maintained at 5°C. The mobile phase consisted of 50mM Phosphate Buffer (pH: 3.0): Acetonitrile (70:30 v/v). The *isocratic* flow rate was 0.75 mL/min. The detection wavelength was 210 nm, bandwidth 4 nm. Injection volume was 20 μ L with the run time of 10 minutes.

6.1.2.3.1 Preparation of Diphenhydramine Stock Solution

Fifty milligrams equivalent (50 mg) of DPH powder was weighed on a Sartorius Analytic lab balance and added to volumetric flask containing approximately 30mL of lactated Ringer's solution (LRS). The volume of the flask was then adjusted to 50 mL to obtain a 1 mg/mL stock solution. Once DPH was dissolved, 25 mL was placed into a 25 mL polypropylene centrifuge tubes and stored in the refrigerator at 4 °C and the other 25 mL was placed into a 25 mL polypropylene centrifuge tubes and stored in the freezer (- 20°C).

6.1.2.3.2 Preparation of Standards

The 1 mg/mL DPH stock solution was removed from the refrigerator and allowed to come to room temperature. A “calibration stock” solution of 100,000 ng/ml of DPH was prepared. Appropriate dilutions were made from the “calibration stock” using LRS to obtain concentrations of 10,000 ng/mL, 5,000 ng/mL, 1,000 ng/mL, 500 ng/mL, 100 ng/mL, and 50ng/mL. The calibrators were prepared in 1.5mL Eppendorf

centrifuge tubes and stored at 4°C then used for one week before being discarded at the end of a week.

6.1.2.3.3 Preparation of Diltiazem Stock Solution

Fifty milligrams equivalent (50 mg) of DTZ powder was weighed on a Sartorius Analytic lab balance and added to volumetric flask containing approximately 30mL of LRS. The volume of the flask was then adjusted to 50 mL to obtain a 1 mg/mL stock solution. Once DTZ was dissolved, 25 mL was placed into a 25 mL polypropylene centrifuge tubes and stored in the refrigerator at 4 °C and the other 25 mL was placed into a 25 mL polypropylene centrifuge tubes and stored in the freezer (- 20°C).

6.1.2.3.4 Preparation of Standards

The 1 mg/mL DTZ stock solution was removed from the refrigerator and allowed to come to room temperature. A “calibration stock” solution of 100,000 ng/ml of DTZ was prepared. Appropriate dilutions were made from the “calibration stock” using LRS to obtain concentrations of 10,000 ng/mL, 5,000 ng/mL, 1,000 ng/mL, 500 ng/mL, 100 ng/mL and 50ng/mL. The calibrators were prepared in 1.5mL Eppendorf centrifuge tubes and stored at 4°C then used for one week before being discarded at the end of a week.

6.1.2.4 Calibration Curve

50µL of each solution of DPH in the concentrations of 10,000ng/mL, 5,000ng/mL, 1,000ng/mL, 500ng/mL, 100ng/mL, and 50ng/mL were withdrawn in different

Eppendorf tubes. 50µL of the DTZ solution in the corresponding concentration was withdrawn and mixed with the respective DPH solutions in the Eppendorf tubes. 20µL of this solution was injected in the HPLC for simultaneous estimation of DPH and DTZ respectively.

The peak areas were used to identify the concentration of the sample. All calibration curves were generated using a weighed 1st degree polynomial linear equation (Phoenix-WNL, Certara, Princeton, NJ). The calibration curve line weighting (1/Y) was used to give equal weight to each of the concentration and peak area output. The slope and y-intercept were used to back-calculate the concentration from the peak area from the calibration curve. Calibration curves of the standards were performed intra-day (n=6) as well as inter-day (n=6) to assess accuracy, precision, linearity as well as the LLOQ.

6.1.2.5 Quality Control (QC) Samples

QCs were prepared from the same stock solution after the stability of the stock solution in the storage conditions had been verified. Each experiment had either 6 QC's (3 concentrations in duplicate – Table 3 & 4) or 5% of the number of samples – whichever was greater. During each run with QC's, at least 75% of the QC's were within 15% of their nominal concentration, while at least 50% of each QC level was within the 15% of nominal concentrations.

Table 3: Quality Control concentrations of DPH used to verify sample analysis

Quality Control Level	Concentration (ng/ml)
High	10000
Middle	500
Low	50

Table 4: Quality Control concentrations of DTZ used to verify sample analysis.

Quality Control Level	Concentration (ng/ml)
High	10000
Middle	500
Low	50

6.1.3 Stability Studies

Bench-top, long-term stability, stock solution stability, freeze-thaw, as well as top-temperature stability was assessed as per the FDA Bioanalytical Guidelines.

6.1.3.1 Bench Top Stability Studies:

Bench-top experiments were performed by analyzing the average of 3 samples from the Low, Middle and High QCs at each time point from t = 0 until 24 hours.

6.1.3.2 Long Term Stability Studies:

Long term stability was performed by comparing the concentrations of standard analyzed just after preparation (fresh) with 6 sets of the same Concentration standards kept in the freezer (-20 °C) for 1 month.

6.1.3.3 Stock Solution Stability Studies:

Stock solution stability was assessed by comparing standards from a fresh stock solution to 6 sets of standards prepared from a stock solution prepared a month prior. 6 sets of Freeze-thaw samples were put in a freezer (-20 °C) for 12 hours, then thawed (4 °C) for 12 hour and repeated the cycle 2 more times and then 6 sets of QCs prepared to be analyzed.

6.1.3.4 Top Temperature Stability Studies:

Top-temperature stability was assessed by average of 3 replicate samples at each hour from Low, Middle and High QCs concentration that are bathed in 37°C for 8 hours, if the percentage error was not greater than 15% - it was considered stable. Since both the drugs DPH and DTZ are analyzed simultaneously, the possibility of chemical interaction between them needs to be tested. A study design was developed where standard solutions for both the drugs were prepared in Lactated ringier's solution individually and in combination to yield the same concentration. Three concentrations 10 µg/ml, 5 µg/ml, and 2.5 µg/ml in triplicates of both DPH and DTZ were prepared to assess the interaction, if any, when mixed in the solution.

6.1.4 Results and Discussion

6.1.4.1 Accuracy and Precision

Accuracy is the closeness of the test results to the true value – in this case the back-calculated concentration to the calculated concentration of the standards. Precision of an analytical method is the degree of the agreement amongst the test results.

Accuracy is expressed as the relative percentage error (%E) while precision is expressed as the coefficient of variation (%CV). According to the FDA Guidelines the maximum %E and %CV allowed for the Lower Limit of Quantification is 20% while it is 15% for all other concentrations. Accuracy and precision of DPH and DTZ was calculated for inter-day (Table 5) and intra-day (Table 6) for DPH and DTZ respectively.

Table 5: Inter-day HPLC method validation of DPH and DTZ in LRS (n=6)

	DPH			DTZ		
Conc (ng/mL)	Mean	STD	%CV	Mean	STD	%CV
10000.00	9984.39	11.35	0.11	10003.11	15.21	0.15
5000.00	5036.45	26.47	0.53	4985.07	25.21	0.51
1000.00	972.27	23.27	2.39	1001.25	37.26	3.72
500.00	500.08	13.47	2.70	497.56	13.85	2.78
100.00	102.87	9.25	8.99	103.05	6.78	6.58
50.00	53.78	7.03	13.07	50.81	7.21	14.19

Table 6: Intra-day HPLC method validation of DPH and DTZ in LRS (n=6)

	DPH			DTZ		
Conc (ng/ml)	Mean	STD	%CV	Mean	STD	%CV
10000.00	10044.73	49.21	0.49	10099.75	38.79	0.38
5000.00	5006.00	56.68	1.13	4925.29	30.66	0.62
1000.00	959.59	26.70	2.78	987.09	24.78	2.51
500.00	489.14	12.05	2.46	488.82	8.92	1.83
100.00	103.42	3.55	3.43	101.25	2.37	2.34
50.00	51.22	1.46	2.84	51.48	2.19	4.25

6.1.4.2 Specificity and Selectivity

Selectivity is the ability of the method to measure the analyte accurately and specifically in the presence of compounds that may also be in the sample matrix.

Specificity of an assay ensures that the signal is the analyte of interest and that it is free from interference from endogenous substances.

Selectivity and specificity were determined by comparing chromatograms of LRS as blank dialysates to those obtained from samples spiked with various concentrations of DPH and DTZ. No interference between matrix and substances was observed. The retention time for DPH and DTZ was 6.5 ± 0.1 and 7.4 ± 0.1 respectively. Examples of chromatogram are presented in Figure 10 and 11.

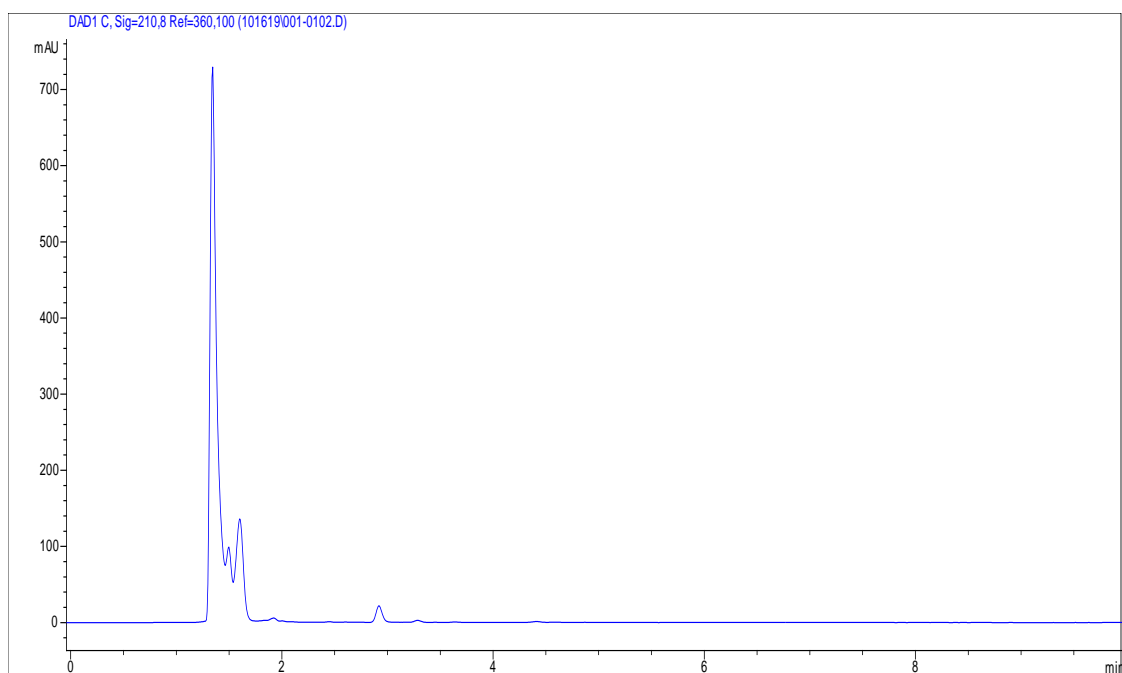


Figure 10: Representative Chromatogram from Agilent 1100 HPLC with DAD detector at $210 \pm 4\text{nm}$ with a reference band at $360 - 100\text{nm}$. Chromatogram for a blank sample: Lactate Ringer Solution

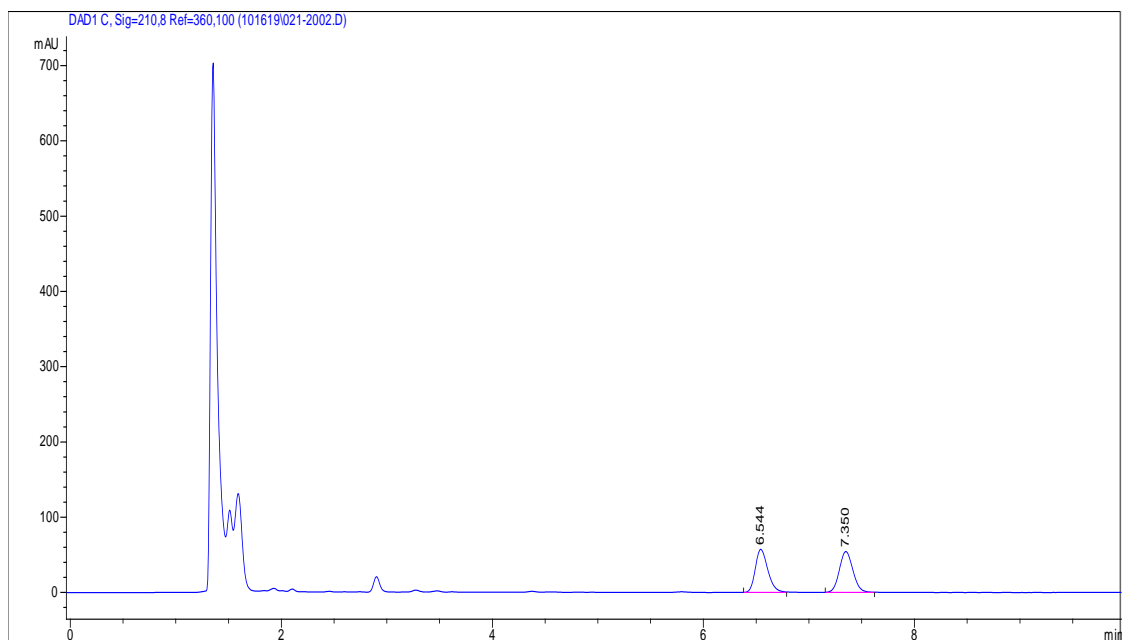


Figure 11: Representative Chromatogram from Agilent 1100 HPLC with DAD detector at $210 \pm 4\text{nm}$ with a reference band at $360 - 100\text{nm}$. Chromatogram for a DPH & DTZ in LRS at peak retention time of 6.5min and 7.4min, respectively.

6.1.4.3 Detection Limit (LOD)

The lowest concentration that can be identified from the noise of the system, although it may have %E or %CV greater than 20% as is difficult to consistently quantify. The LOD in this case is 25ng/ml for DPH and 50ng/ml for DTZ.

6.1.4.4 Quantitation Limit (LLOQ)

The lowest concentration that can accurately and precisely identified. The FDA bioanalytical guidelines specify that the LLOQ cannot have an %E or %CV greater than 20%. The lower limit of quantification for DPH and DTZ was 50ng/ml with an average %E and CV% < 20%.

6.1.4.5 Linearity and Range

The ability of the method to obtain results are related to the linearity of the calibration curve which may be either direct or mathematically transformed, as in our case 1/Y. As previously stated, the line weighting (1/Y) was used to give equal weight to each of the concentration and peak area output. The AUC of DPH in the sample was calculated by an integration method established prior to running samples. The automated integration method was applied for both substances during analysis of samples containing both analytes to determine the linear range of the analytes. Linearity was determined by a plot of the peak areas against the concentrations of DPH and DTZ, which was determined to be 10,000 ng/ml – 50 ng/ml. The correlation coefficient was 0.99 for both APIs.

6.1.4.6 Diphenhydramine Stability

Bench-Top: DPH standards were stable up to 24 hours.

Long Term Stability: DPH was stable up to one month at – 20 °C; Average percentage error for DPH for the frozen High QCs samples was 0.4%, Middle QC was 5.6% and for the Low QCs samples was 17.8% after one month.

Top-Temperature: The mean percentage error for DPH samples kept at 37°C for 8 hours was 1.1%, 3.8% and 12.9% which is < 15% and therefore, DPH is stable for at least 8 hours at 37°C.

Stock Solution Stability: HPLC method was used to determine the stability of the stock solution in a 4°C refrigerator. Results demonstrated that DPH stock solution was stable at least for 1 month when refrigerated and therefore new stock solution was made every month.

Freeze-thaw stability: The average percentage error of the QCs concentration compared with the fresh ones was always within the 15% and thus DPH was stable for three freeze-thaw cycles.

6.1.4.7 Diltiazem Stability

Bench-Top: DTZ standards were stable up to 24 hours.

Long Term Stability: DTZ was stable up to one month at – 20 °C; the average percentage error for the frozen High QCs samples was 0.7%, Middle QC was 3.45% and for the Low QCs samples was 6.89% after one month.

Top-Temperature: The mean percentage error for DTZ samples kept at 37°C for 8 hours was 0.7%, 4.2% and 11.2% which is < 15% and therefore, DTZ is stable for at least 8 hours at 37°C.

Stock Solution Stability: HPLC method was used to determine the stability of the stock solution in a 4°C refrigerator and DTZ stock solution was stable at least for 1 month when refrigerated and therefore new stock was made every month.

Freeze-thaw Stability: The average percentage error of the freeze-thawed samples concentration compared with the fresh for DTZ was within the 15% recommended by the FDA-Guidance.

Table 7 – Summary of HPLC Method validation

Analyte of Interest	Diphenhydramine	Diltiazem
HPLC-UV		
Biological Matrix	Lactated Ringer's Solution	Lactated Ringer's Solution
Calibration Curve Range	10,000-50ng/mL (Matrix A)	10,000-50ng/ml (Matrix B)
Column	ACE Equivalent C18 3.5µm 100 x 4.6mm	
Mobile Phase	Buffer (50mM Phosphate Buffer pH:3.0): Acetonitrile (70:30 v/v)	
Inter-run Accuracy (for each QC Concentration 2replicates) (CV %)	Low QC (50 ng/ml) 13.06% Medium QC (500ng/ml) 2.69% High QC (10000ng/mL) 0.11%	Low QC (50 ng/ml) 14.7% Medium QC (500 ng/ml) 2.7% High QC (10000ng/mL) 0.5%
Top temperature Stability	8 hours at 37°C	8 hours at 37°C
Short Term/ Bench Stability	Stable up to 24 hours	Stable up to 24 hours.
Long Term Stability (Freezer)	Stable for 1 month at -20°C	Stable for 1 month at -20°C
Stock solution stability (Refrigerator)	At least 4 weeks at 4°C	At least 4 weeks at 4°C
Freeze-Thaw Stability	Stable for 3 freeze-thaw cycles of 12 hours/each	Stable for 3 freeze-thaw cycles of 12 hours/each

Table 8 shows the result of back concentration values for DPH and DTZ (single and combination). Both DPH and DTZ were injected separately and together in a mixture and no change in concentration was observed proving that no interaction occurs when dissolved together.

Table 8: Back calculated concentrations for DPH & DTZ

True concentration (µg/ml)	DPH back concentration Single (µg/ml)	DPH back concentration Combination (µg/ml)
10	10.14	10.04
	10.03	9.98
	10.04	10.01
5	5.18	5.01
	4.96	5.04
	5.01	4.96
2.5	2.21	2.52
	2.75	2.43
	2.35	2.61

Table 9 shows the ANOVA single factor analysis (Data analysis tool, MS Excel) for DPH (10 µg/ml) single vs. combination replicates. There were no statistically significant differences between DPH single vs. DPH combination (Concentration 10 µg/ml) as determined by one-way ANOVA ($F(1, 4) = 2.35$, $p = 0.2002$).

Table 9: ANOVA single factor analysis for DPH (10 µg/ml) single vs. combination

ANOVA						
Source of Variation	SS	df	MS	F	P-value	F crit
Between Groups	0.0054	1	0.0054	2.347826	0.200223	7.708647
Within Groups	0.0092	4	0.0023			
Total	0.0146	5				

ANOVA single factor analysis of DPH (single vs. combination) for concentrations 10 µg/ml, 5 µg/ml, and 2.5 µg/ml and DTZ (single vs. combination) for concentrations 10 µg/ml, 5 µg/ml and 2.5 µg/ml were also performed. The results showed no statistically significant differences (5 µg/ml – $p = 0.54$, 2.5 µg/ml – $p = 0.65$) in concentrations of DPH and DTZ when dissolved separately vs. together proving no possibility of chemical interaction between DPH & DTZ.

The bio analytical method should be reliable as the results of the entire study depend on the analysis of the samples. For these reasons, new bio analytical methods for individual drugs and simultaneous estimation of DPH and DTZ were developed and validated. Estimated parameters such as accuracy, reproducibility, sensitivity, and selectivity for the determined linearity range were within the limit as described in FDA guidance for bioanalytical method validation. Diphenhydramine did not show any chemical interaction with Diltiazem. Thus, this combination was selected for further study of this project.

CHAPTER 7: GEL PREPARATION & QUANTITATION

7. Gel Preparation and Quantitation

7.1 Method of gel preparation

A total of six combinations of Gel formulations (each consisting of one drug and one penetration enhancer; R & S – Limonene in three different concentrations) along with one control formulation were prepared using simple high speed shearing method. Table 10 describes the %w/w composition of each gel.

Table 10: Formulation chart representing quantity of each ingredient in %w/w for all DPH gels prepared in-house.

Ingredients	R1	S1	R2	S2	R3	S3	C	R1D	S1D	CD
	R - 1.00%	S - 1.00%	R – 1.75%	S – 1.75%	R - 2.50%	S - 2.50%	Control	R - 1.00%	S - 1.00%	Control
DPH	5%	5%	5%	5%	5%	5%	5%	5%	5%	5%
DTZ	-	-	-	-	-	-	-	5%	5%	5%
Klucel HF Pharm	2%	2%	2%	2%	2%	2%	2%	2%	2%	2%
R - Limonene	1.00%	-	1.75%	-	2.50%	-	-	1.00%	-	-
S - Limonene	-	1.00%	-	1.75%	-	2.50%	-	-	1.00%	-
60%v/v Ethanol	qs	qs	Qs	qs	qs	qs	qs	qs	qs	qs
Total	10 g	10 g	10 g	10 g	10 g	10 g	10 g	10 g	10 g	10 g

Gels were prepared by dispersing compounds (in a sequence of DPH and R & S – Limonene where applicable) in 60%v/v ethanol, then adding the gelling agent: Klucel® (Hydroxy Propyl Cellulose) and applying energy (e.g.: shear force) through mixing until uniform. One formulation without the penetration enhancer was formulated in a similar way as a control. The resulting formulations were then stored at 4°C overnight to ensure complete polymer dissolution. The two formulations with the best drug release profiles were selected for further studies with the calcium channel blocker - DTZ. The two selected formulations containing Limonene were now prepared along with DTZ using the same technique. The gels were stored overnight at room temperature (25°C) before its use. Stability studies were performed for the intended period of use for prepared gels.

7.2 Method for gel quantitation: Drug Content Assay

The drug content assessment is necessary to confirm the uniformity of gel formulation. Approximately, 100mg of the gel (n=6) was weighed and diluted with 1ml of deionized water. The resultant mixture was vortex mixed and centrifuged for 10 minutes at 10000RPM. 50µl of the resulting solution was further diluted with 1ml of deionized water. 50µl of the resulting solution was further diluted with 1ml of deionized water. 20µl of the resulting solution was injected into the HPLC for analysis.

7.3 Results and Discussion

All gel formulations were clear and transparent with no visible color. There was no presence of particles, floccules, or lumps seen in the gels. The results of the drug content test are described in Table 11.

Table 11: Results of quantitation of each gel formulation

Formulations	DPH Concentration ($\mu\text{g/ml}$, mean \pm SD, n = 6)	% Recovery
R1	0.60 \pm 0.03	96.0
S1	0.58 \pm 0.02	92.8
R2	0.56 \pm 0.04	90.9
S2	0.57 \pm 0.03	90.1
R3	0.57 \pm 0.05	91.2
S3	0.61 \pm 0.06	97.6
C (Control)	0.59 \pm 0.06	94.4
R1D	0.60 \pm 0.03	96.0
S1D	0.63 \pm 0.02	100.8
CD (Control + DTZ)	0.59 \pm 0.04	94.4

The results show that all the gels were similar in appearance and had the same visible features. Single factor ANOVA was performed on the DPH recovery concentration which showed that there was no statistically significant difference between DPH recovery amongst individual gels ($p = 0.49$). The drug content in six replicates from various part of the gels have similar concentration, which proves that the ingredients were distributed homogeneously throughout the gel.

CHAPTER 8: IN VITRO RELEASE STUDIES

8. *In vitro* Release Studies

8.1 Purpose

The goal of this proposed dissertation is to test the possibility that the CCB DTZ lowers the PE activity of Limonene on the drug DPH due to a possible interaction with Ca^{2+} ions in the skin. It is thus important to rule out the possibility that DTZ interferes with the release of DPH from the formulation itself. For this reason, the release rate profiles of gels containing DPH alone and DPH with DTZ were investigated *in vitro* using the cellulose membrane and a Franz cell apparatus. The presence of other ingredients should not lower the release rate of the active drug molecules due to any chemical or physical interactions. Cellulose membranes, based on the pore size requirement, have been widely used for *in vitro* diffusion studies in the scientific community. The polymer nature of cellulose membrane provides web like structure which serves as the matrix for the release study. Franz cell apparatus is used widely for the drug release/diffusion studies from various formulations. Franz cell usually consists of donor compartment, receiver compartment, sampling port and two outlets for the heat circulation to maintain the temperature of the receiver compartment if needed. A known amount of formulation is placed in the donor compartment and samples are collected from the sampling port at desired time points. The volume of a withdrawn sample is replaced with an identical volume by the same solution used in the receiver compartment so that the total volume and composition of the receiver compartment remains the same.

The analysis of the samples is performed by plotting the cumulative amount of drug versus time. The parameter such as flux, which is a slope of the straight-line portion of the plot (amount/area/time), and cumulative amount, which is the amount collected at the end of the sampling frequency (amount/area) are calculated to interpret the drug release profile from the formulations.

The cumulative amount released through the cellulose membrane was calculated to compare the release profiles of the formulations and select the best drug release formulation for each of the enantiomer concentrations. In-vitro release study was performed for the gel formulations containing CCB. The release rate parameters (Flux, Cumulative amount) were calculated and compared to see if there were any physical/chemical interactions between the drug, calcium channel blocker and Limonene. Ideally, all three gel formulations should have no significant difference in flux and in total amount released.



Figure 12: Franz diffusion cell apparatus with donor and receptor chamber

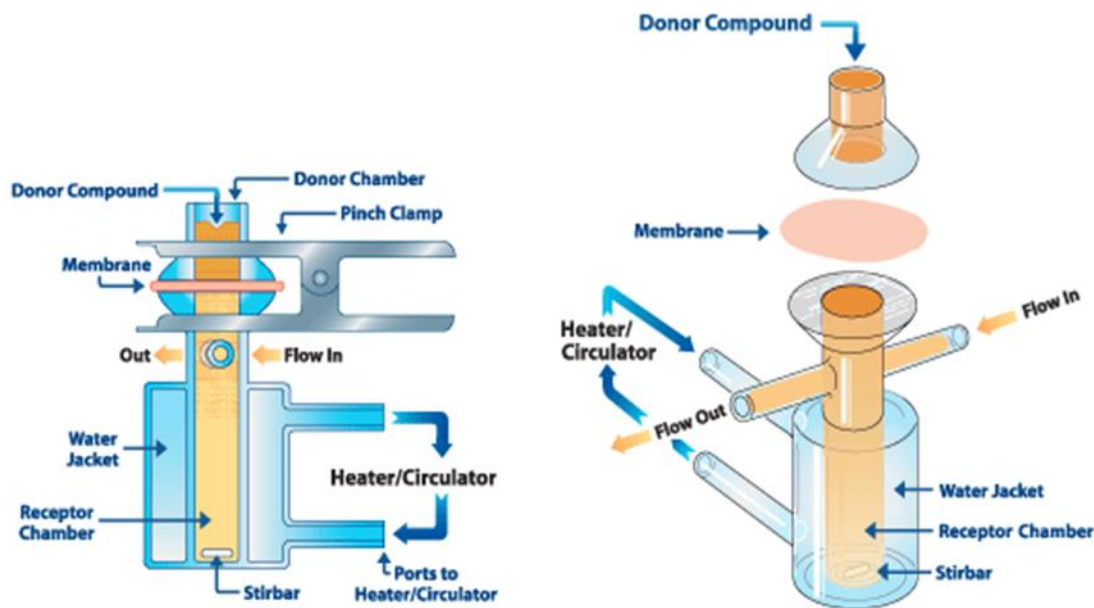


Figure 13: Franz Cell Assembly [50]

8.2 Method

The standard jacketed Type 1 Franz diffusion cell (Figure 12) containing sampling port and Flow port (PermeGear, Inc., Hellertown, PA) with permeable area of 0.95 cm², diameter of 1.1cm and internal volume of 8.9ml was used to perform the *in-vitro* release studies. A Spectra/Por7 (Laguna Hills, CA) regenerated cellulose membrane (60 - 65µm thickness; molecular weight cut-off 1000) saturated in Lactated Ringer solution for 1 hour was placed between the receiver compartment and the donor compartment. A pinch clamp was used to secure the donor compartment to the receiver compartment. The receiver compartment contained Lactated Ringer's solution. The system was maintained at $37 \pm 0.5^{\circ}\text{C}$ by a water bath circulator and a jacket surrounding the cell (figure 13). A TeflonTM coated magnetic bar was used to

continuously stir the receiving medium to avoid diffusion layer effects. The cellulose membrane was immersed in Lactated Ringer's solution for 1 hour prior to mounting on the Franz cell. The open end of the compartment was sealed using an aluminum foil followed by Parafilm to prevent any evaporation of the solvent from the gel formulations. Approximately 50 μ l of receptor fluid was withdrawn from the receiver compartment every 15 minutes for first hour and then every 30 minutes until 6 hours. The volume of every sample withdrawn was replaced by 50 μ l of Lactated Ringer's solution to maintain the constant volume in the receiver compartment. The samples were then injected into HPLC for analysis. Experiments were performed in three replicates.

8.3 Result and discussion

Figure 14 shows the cumulative amount of DPH released over a period of six hours through cellulose membrane and Table 12 reports the release rate parameters such as flux (Amount/(cm²*min)) and cumulative amount for all seven gel formulations. These results show that DPH release was not statistically different (ANOVA) ($F(9,20) = 2.33$, $p = 0.06$) among the tested gel formulations and thus there is no physical interactions between DPH, DTZ, and (R) or (S) limonene.

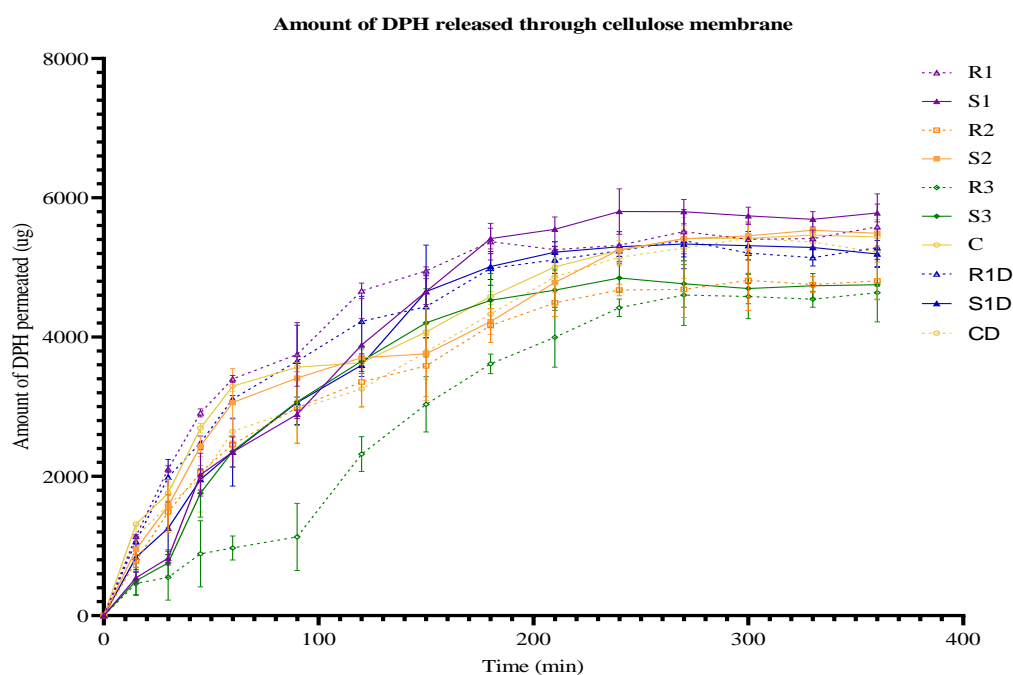


Figure 14: The release rate profiles of DPH for Franz cell diffusion study using cellulose membrane is showed here. Graphical representation of cumulative amount of drug (DPH) released from all seven formulations using cellulose membrane. Each line represents an average of three replicates. The error bars show the standard deviation of the three replicates.

Table 12: Flux and cumulative amount of DPH permeated from three replicates of in vitro release study using cellulose membrane. (mean \pm SD, N=6)

	J ($\mu\text{g cm}^{-2} \text{min}^{-1}$)	Total diffusion after 6h (μg)
R1	27.23 \pm 4.08	5583.53 \pm 472.08
R1D	25.08 \pm 3.35	5284.40 \pm 271.99
S1	29.83 \pm 3.93	5781.82 \pm 129.41
S1D	27.02 \pm 5.04	5191.89 \pm 195.24
R2	20.96 \pm 3.52	4806.70 \pm 271.99
S2	21.05 \pm 3.85	5489.65 \pm 195.24
R3	19.63 \pm 4.09	4636.51 \pm 94.37
S3	26.06 \pm 3.46	4752.55 \pm 533.56
C	21.68 \pm 4.15	5437.83 \pm 30.31
CD	20.98 \pm 3.99	5217.85 \pm 94.37

CHAPTER 9: IN VITRO PERMEATION STUDIES

9. In Vitro Permeation Studies

9.1 Purpose

A successful topical drug delivery product should deliver the active component(s) effectively and in a reproducible way. The optimal composition of the formulation is usually identified by screening the candidate products in-vitro on their capability to deliver the drug across a biological membrane either from human (e.g., cadaver skin) or animal origin (e.g., porcine ear). Here, we used Franz cell apparatus with freshly excised porcine skin to find what concentration of Limonene in the seven formulations of DPH gels results in the higher permeability over a period of six hours. The gel formulation with the highest cumulative amount permeated through the skin and flux were selected for the second part of the project, when a CCB was added to the formulation and tested for permeability and flux.

9.2 Method

Freshly excised porcine ears were obtained on the day of the experiment from a local slaughterhouse. During the transport, the fresh porcine ears were kept at 4°C. The whole ears were then cleaned with warm water to remove bloodstains. The excess water on the skin surface was immediately removed by blotting with Kim wipes. All seven formulations were tested for ex vivo permeation studies.

A full thickness skin of 0.9 - 1.15 mm was separated from the porcine ear by removing the connecting tissues with a surgical scalpel. The integrity of the specimens' skin was checked by visual inspection. No skin samples with wounds

were utilized. An electronic digital caliper was used to measure the thickness of the skin. The skin was hydrated for 1 hour in LRS before the experiment and mounted between receiver and donor compartments of the modified Franz diffusion cells with the stratum corneum side facing the donor compartment. The same experimental set up and procedure described in “Franz cell assembly” was used to perform permeation study through porcine ear skin. Three replicate experiments per gel formulation were conducted.

The cumulative amount of drug permeated ($\mu\text{g}/\text{cm}^2$) through the skin was plotted against time, and drug flux ($\mu\text{g}/\text{cm}^2\text{h}$) was calculated by dividing the slope of the linear portion of the curve with the area of exposed skin surface. The permeability coefficient (cm/h) was derived by dividing the flux obtained from initial drug load.

9.3 Result and discussion

Figure 15 shows the cumulative amount released from the six formulations containing Limonene along with the control. These results show that highest DPH permeability across the porcine ear skin was observed for formulations consisting of 1% R-L and 1% S-L as compared to the formulations consisting of 1.75 and 2.5% limonene. Hence, these formulations were further prepared along with CCB: DTZ and tested for permeability parameters using Franz cell apparatus and porcine ear skin model.

Table 13 reports the permeability parameters such as flux ($\text{Amount}/(\text{cm}^2 \cdot \text{min})$) and cumulative amount for all seven gel formulations. ANOVA for these flux results show that amount of DPH permeated through the porcine ear skin for R1 ($F(1,4) =$

2681.11, $p = 8.3\text{E-}07$) and S1 ($F(1,4) = 2834.93$, $p = 7.4\text{E-}07$) were found to be statistically different when compared to the control formulation.

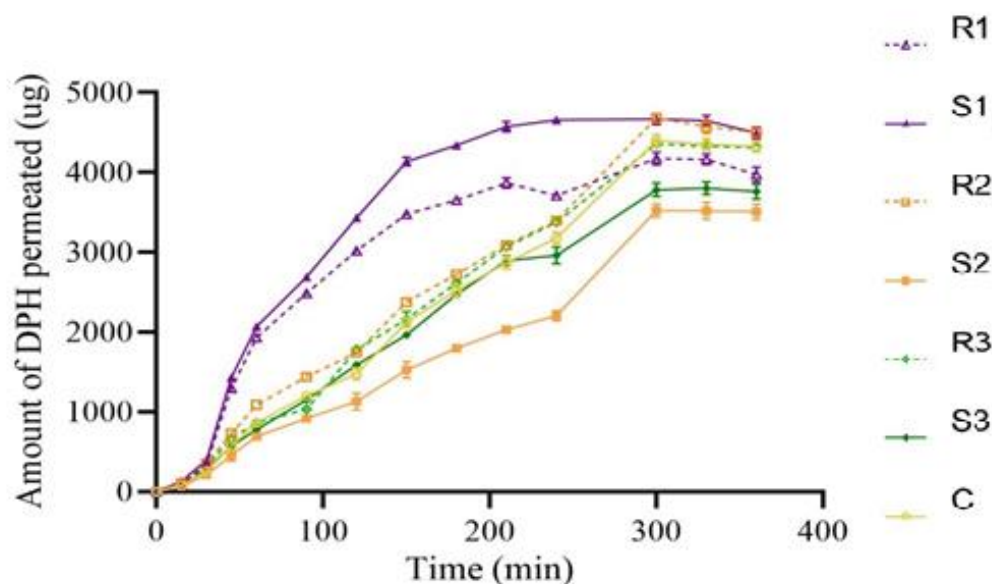


Figure 15: Time course of cumulative amount of drug (DPH) released from all seven formulations using porcine ear skin is showed here. Each line represents an average of three replicates. The error bars show the standard deviation of the three replicates.

Table 13: Flux (J), cumulative amount permeated after 6h and permeability coefficient (K_p) values from three replicates of in vitro permeation studies using porcine ear skin. (mean \pm SD, $N=6$)

	Cumulative amount of DPH permeated after 6h (μg)	J ($\mu\text{g cm}^{-2} \text{min}^{-1}$)	K_p (cm min^{-1})
R1	3973.63 ± 94.07	25.33 ± 0.11	5.07 ± 0.02
S1	4491.75 ± 71.09	29.41 ± 0.35	5.88 ± 0.07
R2	4500.55 ± 46.94	15.14 ± 0.13	3.03 ± 0.03
S2	3506.81 ± 94.41	9.98 ± 0.21	1.99 ± 0.04
R3	4310.35 ± 39.45	14.72 ± 0.09	2.94 ± 0.02
S3	3761.08 ± 92.34	14.05 ± 0.18	2.81 ± 0.04
C	4325.85 ± 71.39	13.88 ± 0.37	2.78 ± 0.07

Figure 16 shows the comparison of cumulative amount of DPH released from all six formulations (three without CCB and three with CCB). These results show that DPH permeability across the porcine ear skin decreased with addition of CCB DTZ in both 1% R-L and 1% S-L formulations. Addition of DTZ to the formulations R1 ($p = 0.0006$) and S1 ($p = 0.0002$) significantly decreased the permeability coefficient of the formulation by 37.08% and 19.56%, respectively.

Amount of DPH permeated through porcine ear skin in presence of DTZ

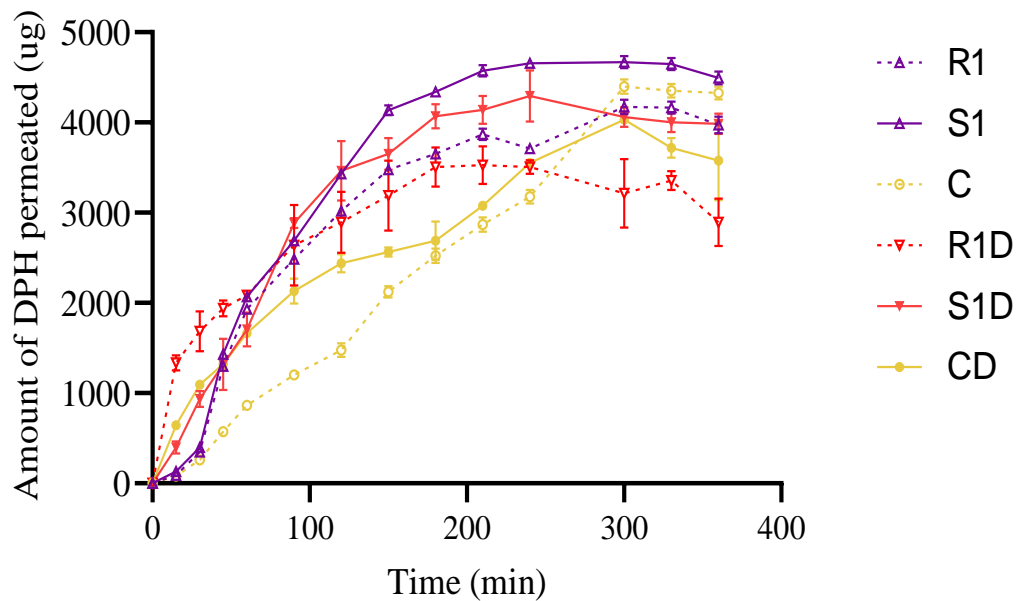


Figure 16: Time course of cumulative amount of drug (DPH) released from all six formulations (three formulations without CCB and three containing CCB) using porcine ear skin is showed here. Each line represents an average of three replicates. The error bars show the standard deviation of the three replicates.

Table 14: Flux (J), cumulative amount of DPH permeated after 6h and permeability coefficient (Kp) values from three replicates of in vitro permeation studies using porcine ear skin for formulations with and without 1% R-L and S-L. (mean \pm SD, N=6)

Formulations	Cumulative amount of DPH permeated after 6h (μg)	J ($\mu\text{g cm}^{-2} \text{ min}^{-1}$)	Kp (cm min^{-1})
R1	3973.6 \pm 94.07	25.33 \pm 0.11	5.07 \pm 0.02
S1	4491.7 \pm 71.09	29.41 \pm 0.35	5.88 \pm 0.07
C	4325.8 \pm 71.39	13.88 \pm 0.37	2.78 \pm 0.07
R1D	2894.7 \pm 264.17	15.98 \pm 1.64	3.19 \pm 0.33
S1D	3986.2 \pm 113.78	23.63 \pm 0.64	4.73 \pm 0.13
CD	3578.0 \pm 439.77	15.73 \pm 0.56	3.15 \pm 0.11

Table 14 reports the permeability parameters such as flux (Amount/($\text{cm}^2 \cdot \text{min}$)) and cumulative amount for six gel formulations (three without CCB and three with CCB). ANOVA for these flux results show that amount of DPH permeated through the porcine ear skin for R1D ($F(1,4) = 97.60$, $p = 0.0006$) and S1D ($F(1,4) = 188.39$, $p = 0.0002$) were found to be statistically different when compared to their respective formulations without CCB suggesting inhibition of Limonene induced permeation due to presence of DTZ.

CHAPTER 10: IN VITRO MICRODIALYSIS

10. In vitro microdialysis

10.1 Purpose

The properties (such as pKa, lipophilicity, or molecular weight) of substrates being analyzed greatly affect its recovery with the microdialysis technique. *In-vitro* microdialysis studies should be conducted to evaluate the suitability of a given microdialysis technique for the desired drug molecule. Also, because the perfusate is constantly perfused through the microdialysis probe, equilibrium between the analyte concentration in the dialysate and the surrounding fluid is never achieved. Relative recovery should be estimated and used to assess the actual concentration of drug in the peripheral interstitial fluid. Diffusion process is considered to be equal in either direction of the semipermeable membrane. Experiments involving gain and loss need to be performed to further confirm that diffusion is indeed direction independent. *In vivo* recovery (gain) is carried out by passing Lactated ringer's solution through the semipermeable membrane surrounded by a solution containing analytes. Dialysates are then analyzed in HPLC and % gain is calculated as per equation 1. Retro dialysis is carried out by passing drug solution in perfusate surrounded by Lactated ringer's solution and %loss is calculated using equation 2.

$$\%Gain = \frac{C_{Dialysate}}{C_{Solution}} \times 100 \dots \dots \dots \text{Equation 1}$$

$$\%Loss = \frac{C_{Perfusate} - C_{Dialysate}}{C_{Perfusate}} \times 100 \dots \dots \dots \text{Equation 2}$$

Three replicates were carried out using three different concentrations to calculate %gain and %loss for diphenhydramine and results should prove that %gain is equal to %loss (Plock and Kloft 2005, Stagni 2011).

10.2 Method

10.2.1 In-house probe manufacturing procedure

- A full piece of polyimide tubing (12 inches) was cut into four equal arms by cutting the entire piece in half and then the two pieces were again cut in half.
- The semipermeable membrane (Gambro AN69 fiber) was measured and cut to the desired length (1.7 cm plus a few mm extra in order to have space to insert the polyimide arms).
- Approximately 25 cm long stainless-steel wire (0.05mm diameter) was measured and cut.
- The cut stainless steel wire was inserted into one polyimide arm. Then the stainless-steel wire was inserted through the pre-cut semi-permeable membrane and then the second polyimide arm.
- Push the polyimide arms through the semi-permeable membrane and ensure the membrane window of the correct length (1.7cm).
- Apply glue with a needle on the connection between the arms and the membrane.
- Wipe away excess glue so that the membrane does not get blocked. Cut the excess stainless-steel wire on the ends and allow to air dry for approximately 30 minutes before using or packaging.

10.2.2 In vitro Microdialysis & Retrodialysis Method

Three probes were placed in a jacketed beaker (maintained at $37 \pm 0.5^{\circ}\text{C}$ with a water bath circulator) and taped to the border of the beaker (Figure 17) so that the membranes were at least 1cm apart. For %Gain (Microdialysis) studies, the beaker was filled with DPH in lactate Ringer (LRS) of 10, 5, or $1\mu\text{g/ml}$ and DTZ of 10, 5, or $1\mu\text{g/ml}$ in LRS solutions in separate experiments and in the presence of each other in concentration of 10, 5, or $1\mu\text{g/ml}$, and the probes were perfused with LRS at $1\mu\text{L/min}$. The dialysate (liquid collected after passing through the concentrated drug solution) was collected every 60 minutes and then analyzed by HPLC method. The probe will “pick-up” the analyte and the concentration that is in the dialysate is compared to the bulk concentration to calculate the % Gain. Figure 18 shows a schematic representation of the experimental set-up.

For % Loss (Retrodialysis) studies the drug solution (10, 5, or $1\mu\text{g/ml}$) was perfused separately and in the presence of each other through the probes and the beaker was filled with plain LRS. The amount of drug that is in the dialysate is analyzed and compared to the concentration of drug in the syringe using the following equations. %Gain and %loss studies were completed using HPLC method.

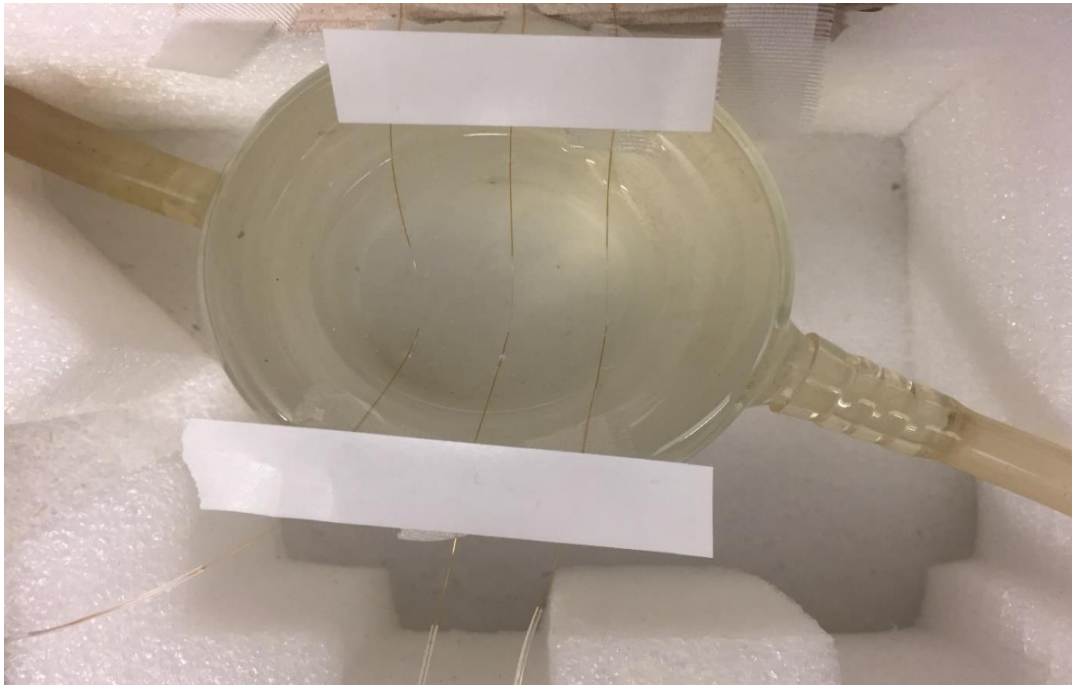


Figure 17: In vitro assembly set up shows the probe spacing in the jacketed cylinder.

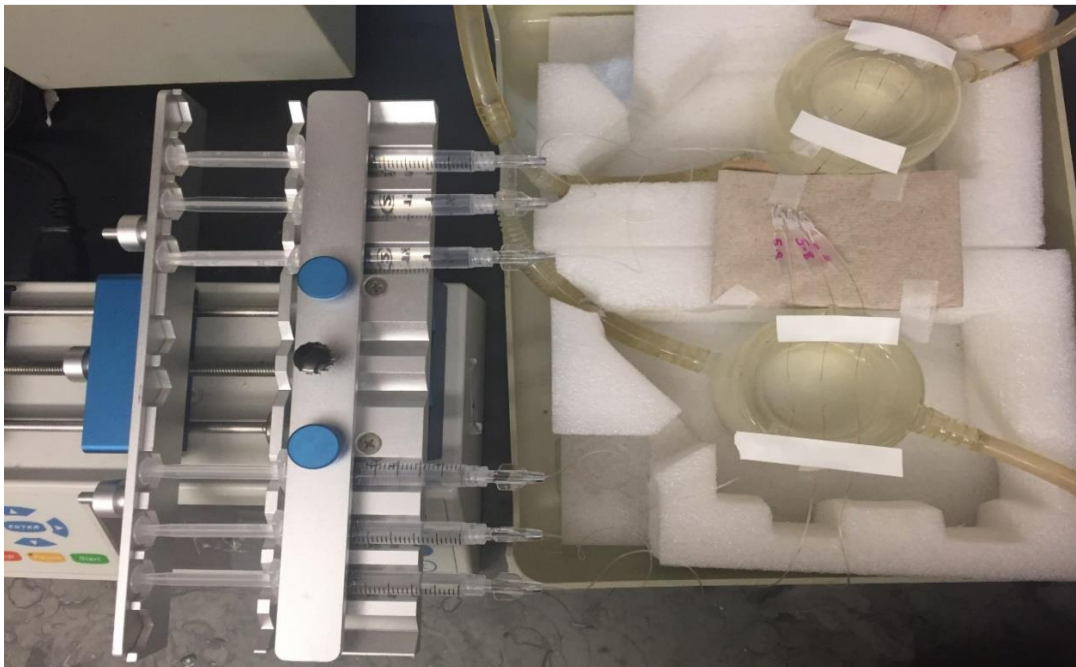


Figure 18: In vitro assembly set up: Shows the entire assembly set up for Gain and Loss experiments.

10.3 Results and discussions

Assessment of %gain in the dMD probes was performed by placing the probes in jacketed beakers containing 1, 5, and 10 µg/mL DPH bulk solutions, with circulation water at 37 ± 0.5 °C, as illustrated in fig 18, (n=3). The perfusate was perfused at 1.0µL/min. The %gain of DPH from bulk solution at different concentrations shows a linear relationship (Figure 19). The results of these experiments demonstrate the suitability of microdialysis technique for DPH. As we can see in the table 15 and 16, the *in-vitro* %gain and %loss values of DPH were near equal proving that diffusion of DPH was direction independent. Thus, proving that DPH was a good candidate for dermal microdialysis technique.

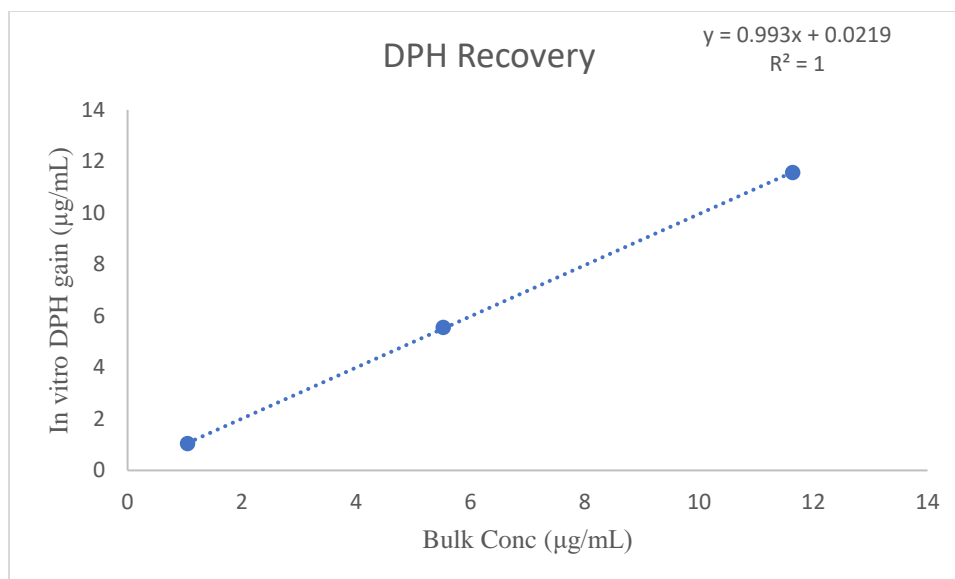


Figure 19: Linear relationship of Steady State Recovery of DPH from bulk in vitro at three different concentrations (1, 5 and 10 µg/mL). (Mean \pm SD, n=3).

Table 15: Results of in vitro % gain experiments for DPH and DTZ (mean \pm SD, N = 3)

Concentration ($\mu\text{g/ml}$)	% Gain			
	DPH Single	DPH Combination	DTZ Single	DTZ Combination
10	96.76 \pm 1.54	94.97 \pm 3.93	100.66 \pm 0.93	83.15 \pm 10.90
5	99.54 \pm 1.79	92.97 \pm 3.71	95.35 \pm 6.12	96.80 \pm 12.22
1	100.9 \pm 2.69	98.10 \pm 2.95	95.01 \pm 10.15	91.90 \pm 3.88

Table 16: Result of in vitro % loss experiments for DPH and DTZ (mean \pm SD, N = 3)

Concentration ($\mu\text{g/ml}$)	% Loss			
	DPH Single	DPH Combination	DTZ Single	DTZ Combination
10	94.88 \pm 3.35	95.70 \pm 3.35	95.13 \pm 1.18	84.07 \pm 1.02
5	98.67 \pm 0.09	94.79 \pm 3.50	98.92 \pm 0.29	93.77 \pm 7.44
1	93.70 \pm 1.21	95.84 \pm 2.45	98.43 \pm 0.32	90.86 \pm 7.36

CHAPTER 11: IN VIVO STUDIES

11. In vivo experiments:

11.1 Purpose

A significant downside of *in vitro* studies using animal cells is their failure to capture the inherent complexity of organ systems. For example, *in vitro* models might not account for interactions between cells and biochemical processes that occur during turnover and metabolism. The use of animals in *in vivo* studies addresses many of these drawbacks of *in vitro* studies and makes it ‘more translatable’ to humans.

An important aspect of this research is activation of TRP channels in the keratinocytes. All TRP channels have some Ca^{2+} influx activity that is a component of their regulation of diverse cellular processes, except TRPM4 and TRPM5. TRPA1 channels serve as sensors for a variety of environmental factors. When a TRPA1 channel is activated by constituents (molecules/proteins/enzymes in a specific signaling cascade), it triggers immediately Ca^{2+} influx via oxidative phosphorylation pathway [51]. *In vivo* studies were crucial for us to attest the hypothesis that Limonene’s interaction with TRPA1 channel decreases the extracellular Ca^{2+} concentration leading to loosen cell-cell adhesion, thereby increasing intercellular permeation of the active drug DPH.

There are two types of animals used in research studies, small animals like rats, mice, and rabbits and large animals like pigs, dogs, and primates. The small animals are easy to handle and thereby give us more control of the experimental procedure. Rabbits are docile and non-aggressive in nature. Since *in vivo* experiments required a

large surface area for multiple gel applications, rabbits were chosen as the preferred candidate for the in vivo studies.

11.2 Method (dMD Study Design)

In vivo experiments were performed in female, pathogen-free New Zealand albino rabbits weighing 3.5 – 5 kg under the protocol and guidelines approved by the Institution Animal Care and Use Committee (IACUC) at Long Island University, Brooklyn, New York. The rabbits were held under standard laboratory conditions, fed normal chow, and given regular tap water for drinking.

A large area of the rabbit's dorsum was shaved a day before the experiments with the help of an electrical animal hair clipper. The skin was checked for any cuts or wounds caused by the clipper using a magnifying glass before the application of the gels. Linear dMD probes were prepared in-house 24h prior to use. The rabbits were tranquilized with an intramuscular injection of 1 mg/kg midazolam injection. 1 mL (10mg/cm² of DPH) of all four gels (DPH, DPH + DTZ, DPH + R-L/S-L, DPH + R-L/S-L + DTZ) were applied simultaneously on the same rabbit to avoid fluctuations due to room temperature, humidity, and diurnal variation of rabbit (Figure 20). Microdialysis probes were inserted as superficially as possible using a hypodermic needle (25G X 1.5 in) as a guide cannula into the shaved dorsal skin of the rabbit. Two probes were inserted under each gel patch area (figure 21 - 2.5cm) for a total of eight probes (4 gel patches) and an extra one was inserted in the dorsal shaved area of the rabbit to estimate redistribution of the drug in the skin. These probes were

connected to the pump via a Tygon tubing after allowing about 30 – 45 minutes for the rabbit skin to recover from the needle and probe insertion. TEWL measurements were collected for each probe at the application sites as a measure of skin barrier integrity. The flow rate of the pump was maintained at 1 μ l/min and sampling frequency was every 30 minutes resulting in a 30 μ l sample volume; 20 μ l out of the total 30 μ l sample volume was injected in the HPLC for the analysis. The in-vivo experimental set up showing gel application areas is illustrated in Figure 22. A baseline sample was taken (blank) before the beginning of the experiments to verify the specificity of the assay. Average dermatological drug concentration profiles from six probes (three rabbit studies) were then compared between four gels using parameters such as C_{\max} and AUC.

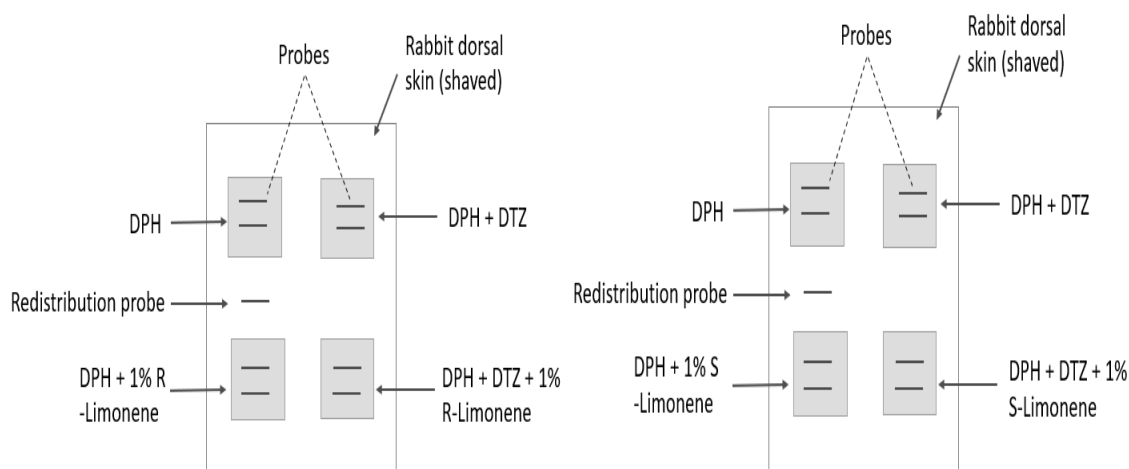


Figure 20: Schematic representation of Rabbit model for In vivo MD study design showing position of microdialysis probes and gel application areas.

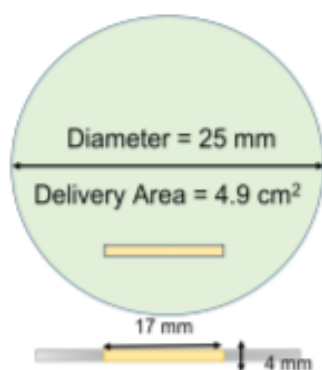


Figure 21: Probe application gel patch area with a diameter of 2.5 cm

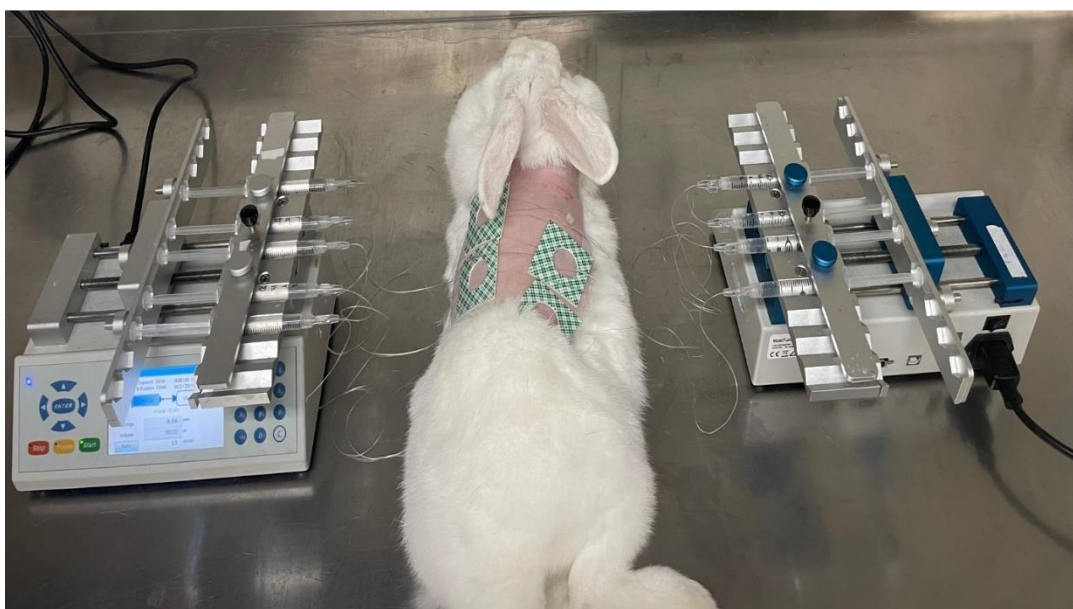


Figure 22: In vivo experimental set-up showing gel application areas on the shaved rabbit dorsum

11.3 Results and Discussion

No interference of any endogenous substances with either DPH or DTZ was found in the sample analysis of in-vivo experiments. The redistribution probe did not detect any DPH concentrations, illustrating there was no redistribution of DPH from the blood to the skin, therefore the dermal concentration of DPH was solely due to DPH permeated from the topical application.

The dermal DPH concentration (ng/mL) profiles are reported below. Figure 23 shows the average DPH dermal concentrations at the same application site from the three rabbits. Figure 24 shows the average dermal concentrations of DPH sorted by rabbit.

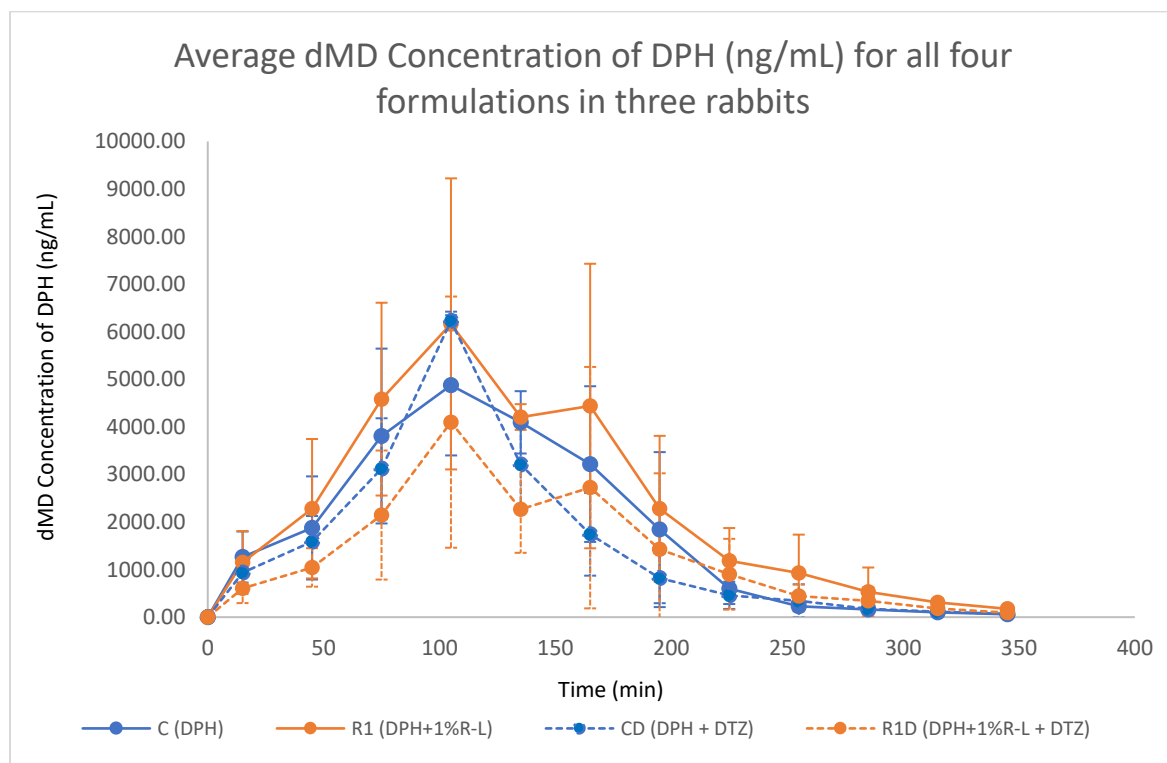


Figure 23: Concentration-time profiles of DPH in dermis after topical administration of four gel formulations (DPH + DTZ(CD), DPH (C), DPH + 1% R-L (R1), DPH + DTZ + 1% R-L (R1D)) on shaved dorsal skin of three rabbits. Vertical bars represent standard deviation of six probes from three rabbit studies.

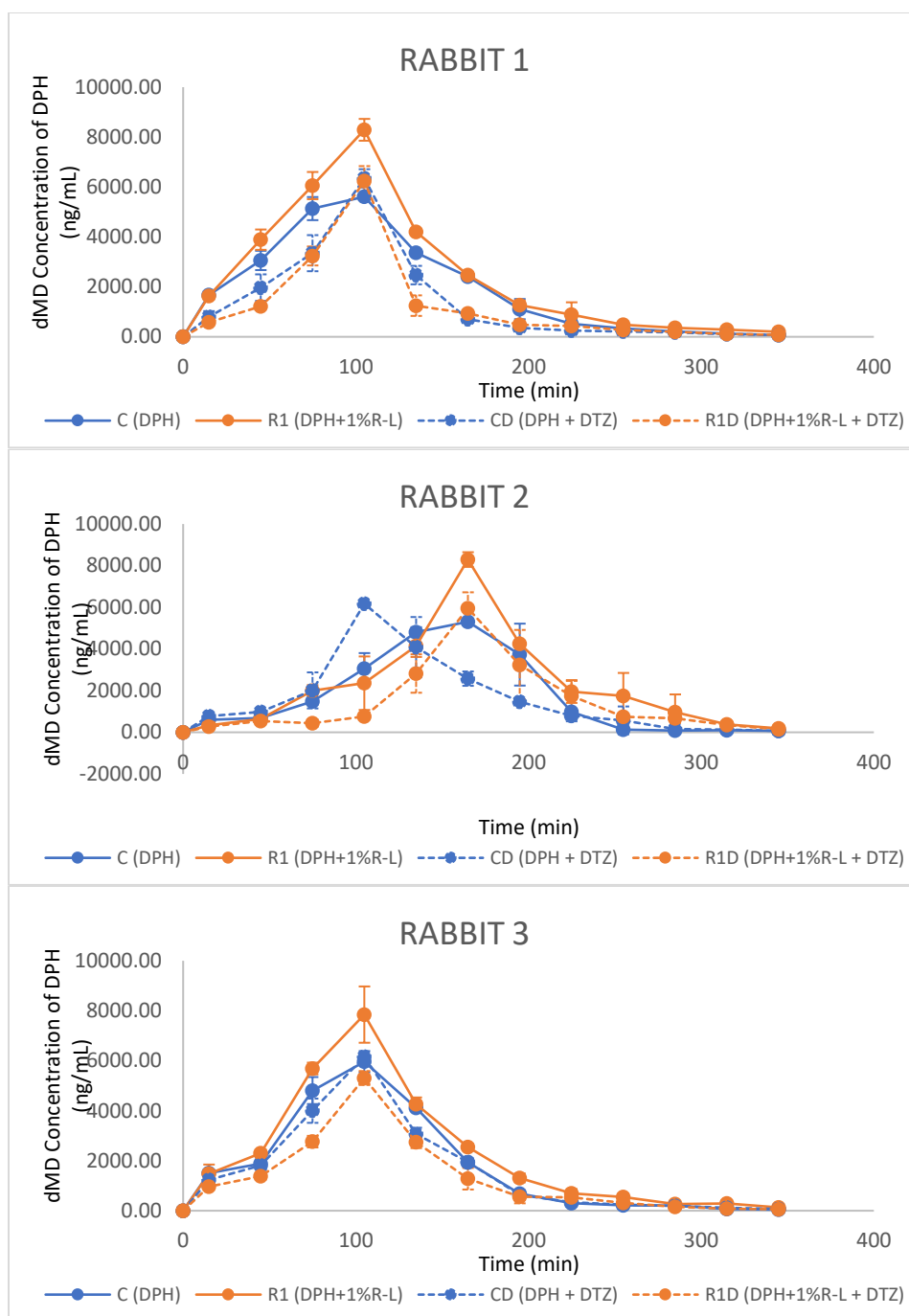


Figure 24: Average dermal Concentration-time profiles of DPH after topical administration of four gel formulations (DPH + DTZ(CD), DPH (C), DPH + 1% R-L (R1), DPH + DTZ + 1% R-L (R1D)) on shaved dorsal skin of three rabbits: (A) – Rabbit 1, (B) – Rabbit 2, (C) – Rabbit 3. Vertical bars represent standard deviation of two probes within the same rabbit.

The maximum dermal concentration of DPH was always higher in the probes at the site of DPH + R-L gel compared to other gels in the same rabbit (figure 25). It was also observed that the increase in Cmax was inhibited when DTZ was added to the gels. The AUC graph (figure 26) represents the total dermal exposure of DPH at the site of application. As we can see from the AUC graph (figure 26) of all four formulations, R1D formulation shows the least DPH permeation through the skin. The skin profile trends are consistent in all three rabbits. This suggests that R-limonene induced penetration enhancing effects on DPH are blocked by DTZ.

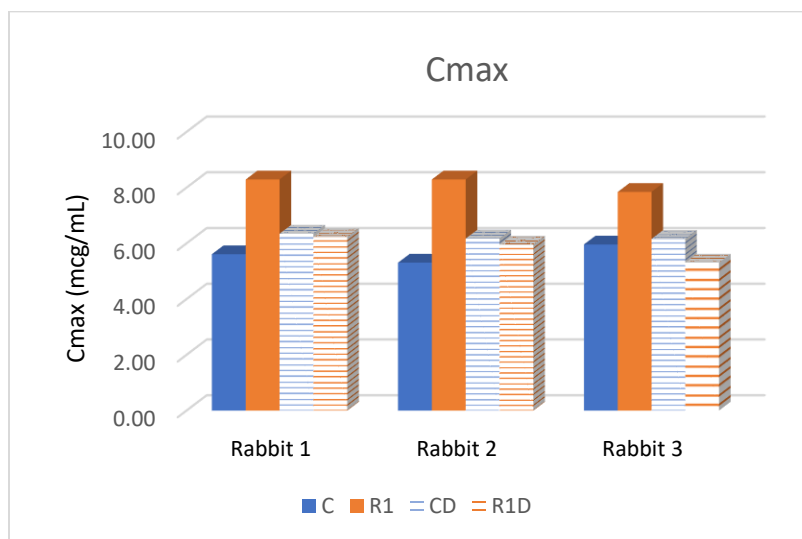


Figure 25: Maximum dermal concentration of DPH in the three rabbits from all gel formulations. C: Control DPH, CD: Control DPH + DTZ, R1: DPH + 1% R-L, R1D: DPH + 1% R-L + DTZ.

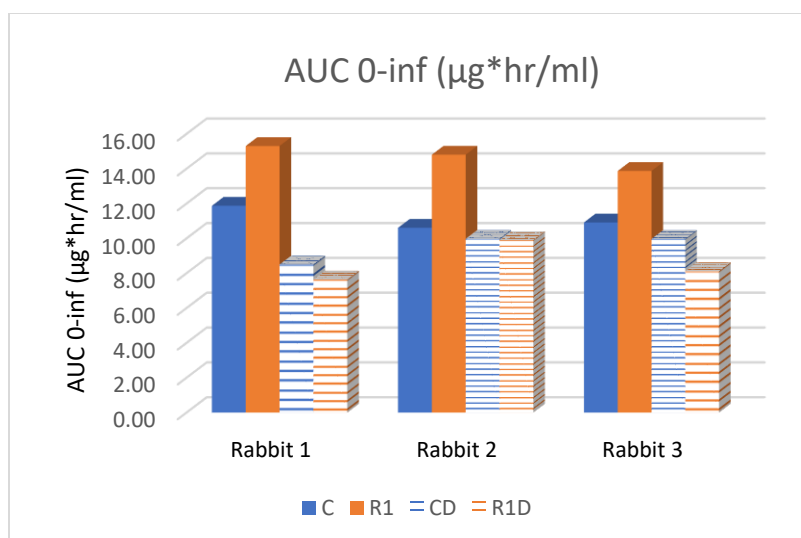


Figure 26: Total dermis exposure of DPH in all three rabbits from all four gel formulations C: Control DPH, CD: Control DPH + DTZ, R1: DPH + 1% R-L, R1D: DPH + 1% R-L + DTZ.

Figure 27 shows the average DPH dermal concentrations when testing the effect of S-L, whereas figure 28 shows the DPH dermal concentrations sorted by rabbit. The average maximum dermal concentration of DPH for three rabbits (six probes) was higher in the probes at the site of DPH + S-L gel compared to other gels (figure 27). While this was also observed for two of the three rabbit studies, one of the probes in the third rabbit study did not show increased permeation of DPH. While average maximum DPH dermal concentration in this rabbit was slightly less than other gel formulations, the AUC was still slightly higher compared to S1D, showing higher exposure of drug from S1. The average dermal concentration skin profile trends are in trend with R-L skin profiles. This suggests that S-limonene induced penetration enhancing effects on DPH might be blocked by DTZ. Since, one probe for rabbit 3 at

S1 site does not show increased penetration, more rabbit studies might be needed to support the hypothesis.

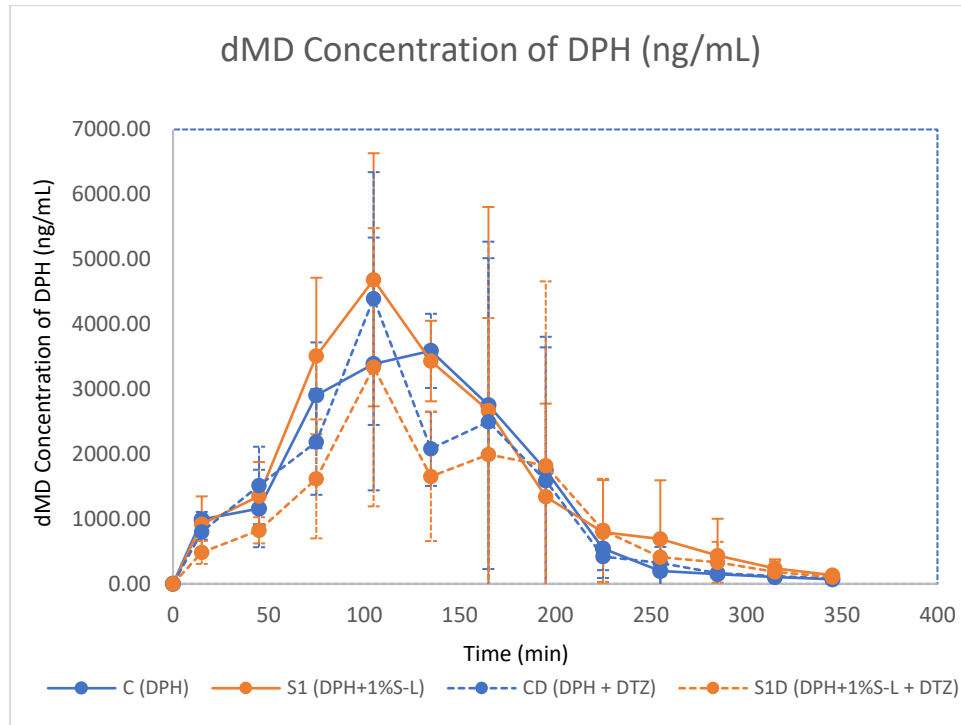
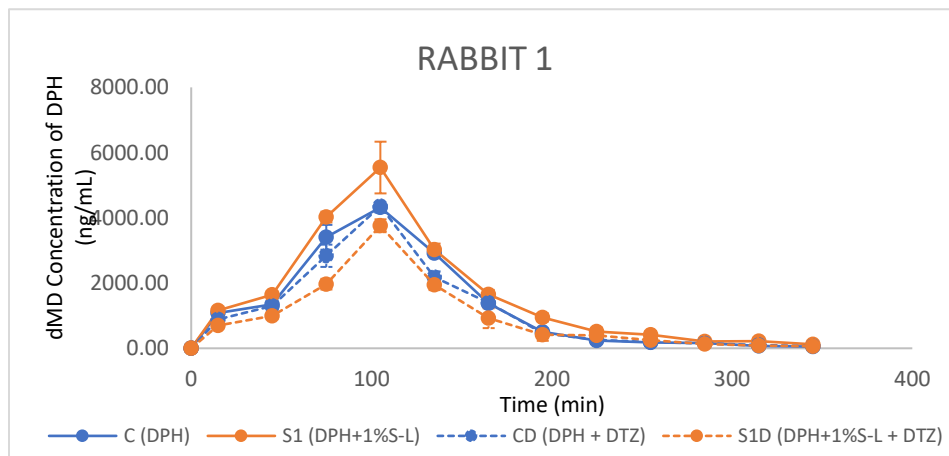


Figure 27: Concentration-time profiles of DPH in dermis after topical administration of four gel formulations (DPH + DTZ, DPH, DPH + 1% S-L (S1), DPH + DTZ + 1% S-L (S1D)) on shaved dorsal skin of three rabbits.



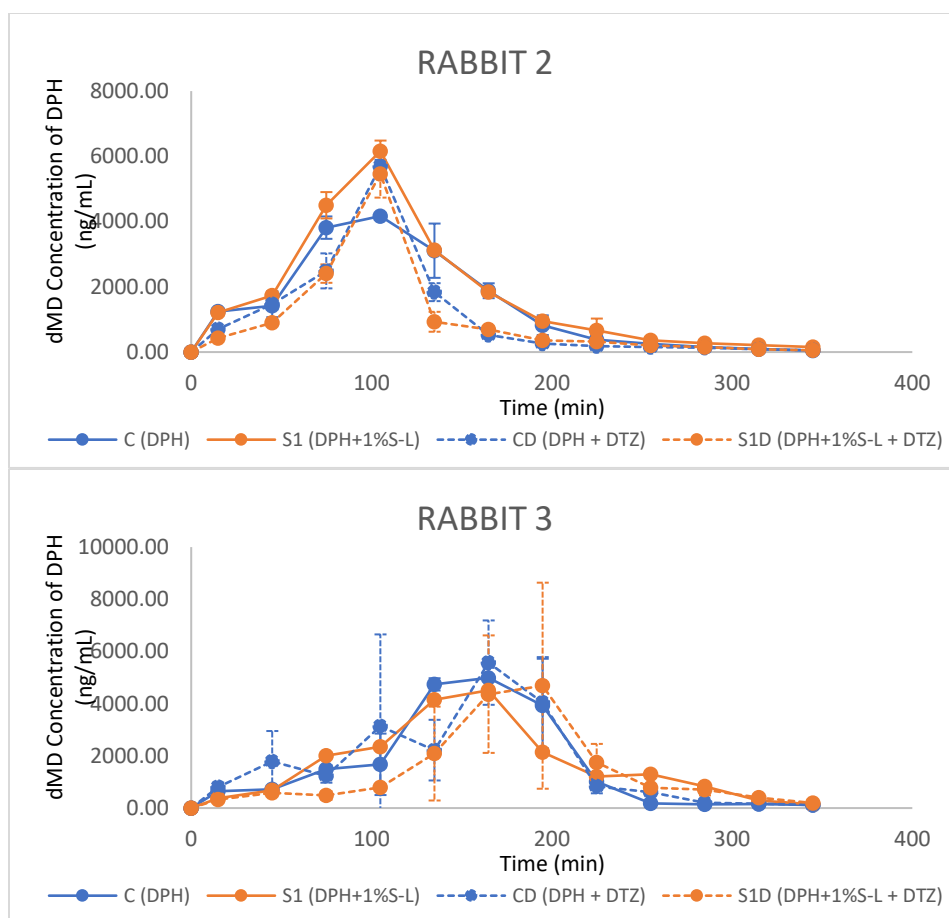


Figure 28: Average dermal Concentration-time profiles of DPH after topical administration of four gel formulations (DPH + DTZ(CD), DPH (C), DPH + 1% S-L (S1), DPH + DTZ + 1% S-L (S1D)) on shaved dorsal skin of three rabbits: (A) – Rabbit 1, (B) – Rabbit 2, (C) – Rabbit 3. Vertical bars represent standard deviation of two probes within the same rabbit.

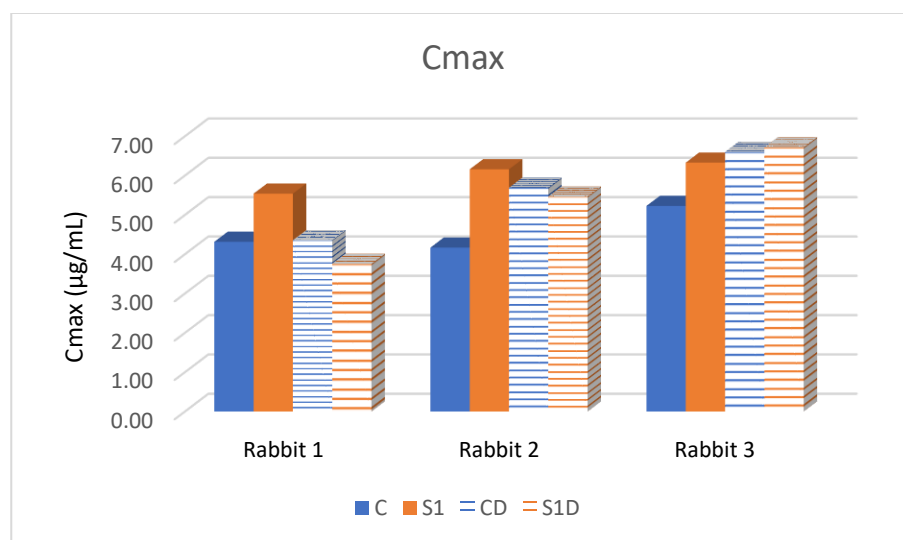


Figure 29: Maximum dermal concentration of DPH in all three rabbits from all gel formulations C: Control DPH, CD: Control DPH + DTZ, S1: DPH + 1% S-L, S1D: DPH + 1% S-L + DTZ.

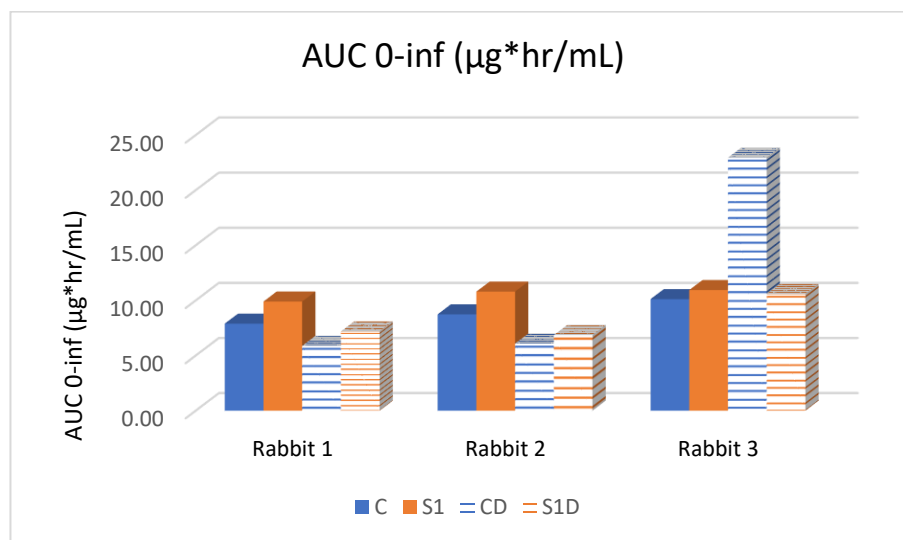


Figure 30: Total dermis concentration of DPH across time in all three rabbits from all four gel formulations C: Control DPH, CD: Control DPH + DTZ, S1: DPH + 1% S-L, S1D: DPH + 1% S-L + DTZ

According to CFR Title 21 Part 320, BE is defined as the absence of a significant difference in the rate and the extent to which the active moiety becomes available at the site of drug action when administered at the same molar dose under similar conditions in an appropriately designed study. MD technique provide a means to

evaluate topical drug penetration of different formulations by continuous sampling and thus provide real-time PK. MD drug penetration data with the test and reference have been obtained in the same subject using a randomized, crossover, single-dose, four treatment study design, thus reducing the intersubject variability. This approach is likely to reduce the number of subjects that would be required to establish topical BE. [52].

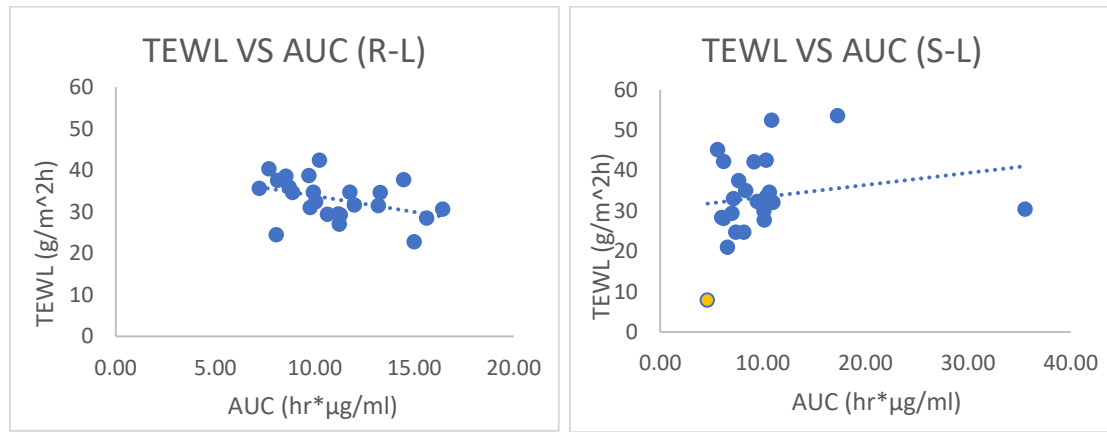


Figure 31: TEWL vs AUC for all six rabbit studies.

Table 17: In vivo comparison of the primary endpoint for test and reference DPH gels

Formulation		R	T/R	90% CI*	R	T/R	90% CI*
Test-R1		C_{max} – 8.14			AUC_{inf} – 14.66		
Reference	C	5.63	1.45	1.2980 – 1.6111	11.13	1.32	1.2101 – 1.4294
	CD	6.23	1.31	1.2361 – 1.3779	9.48	1.55	1.3884 – 1.7309
	R1D	5.83	1.40	1.2454 – 1.5726	8.06	1.72	1.5266 – 1.9405
Test-S1		C_{max} – 6.01			AUC_{inf} – 10.55		
Reference	C	4.57	1.28	0.9806 – 1.6613	8.92	1.11	0.7714 – 1.5975
	CD	5.55	1.06	0.8401 – 1.3452	11.64	1.22	0.8456 – 1.7724
	S1D	5.31	1.10	0.8258 – 1.4698	8.21	1.12	0.5918 – 2.1040
Test-R1D		C_{max} – 5.83			AUC_{inf} – 8.55		
Reference	C	5.63	1.03	0.9272 – 1.1516 ^a	11.13	0.76	0.6813 – 0.8570
	CD	6.23	0.93	0.8497 – 1.0234 ^a	9.48	0.90	0.7889 – 1.0282
	R1	8.14	0.71	0.6359 – 0.8030	14.66	0.58	0.5153 – 0.6550
Test-S1D		C_{max} – 5.31			AUC_{inf} – 8.21		

Reference	C	4.57	1.15	0.9467 – 1.4177	8.92	0.99	0.5467 – 1.8104
	CD	5.55	0.96	0.8744 – 1.0648 ^a	11.64	1.10	0.5919 – 2.0336
	S1	6.01	0.91	0.6804 – 1.2109	10.55	0.90	0.4753 – 1.6897

*90% CIs for the ratio of the means (test/reference) of the listed parameters.

^a Can claim equivalence with the corresponding reference gel formulation.

Table 18: Grouping Information Using the Tukey Method and 95% Confidence (N=6)

Factor	Mean C _{max}	Grouping		Factor	Mean AUC _{inf}	Grouping		
R1	8.142	A		R1	14.661	A		
C	5.625		B	C	11.133	A		
CD	6.228		B	CD	9.483	A		
R1D	5.833		B	R1D	8.552	A		
<i>Means that do not share a letter are significantly different.</i>								
S1	6.010	A		S1	10.55	A		
C	4.572	A		C	8.918	A		
CD	5.551	A		CD	11.64	A		
S1D	5.313	A		S1D	8.205	A		

Two sample equivalence test was performed using minitab to determine the statistical significance of the results. Two formulations containing R-L/S-L with and without DTZ were compared to the reference (C/CD) in the in vivo rabbit model. Analogous to the procedure used in oral bioequivalence studies, test and reference products were compared with respect to two primary endpoints: total drug exposure (AUC, µg*hr/ml), maximum rate of absorption/permeation (C_{max}, µg/mL). Mean grouping using Tukey's method and 95%CI was also performed to identify the equivalency amongst the group means. Maximum dermal exposure (C_{max}) observed at the R1 (R-L) gel was higher than those observed at the other gel sites whereas the addition of diltiazem (R1D) returned exposure to the control level offsetting the PE capacity of Limonene. R1D was found to be equivalent to C (p = 0.008) & CD (p = 0.010),

whereas R1D was not found equivalent to R1 ($p = 0.946$). Results observed with formulations containing S-L (figure 27, 28, 29 & 30) showed higher maximum dermal concentration for two rabbits, while third rabbit showed significantly lower permeation at one of the probes at S1 location. This could have been due to the severely low TEWL at the site. It is unusual to see wide difference in TEWL at same location with two probes, however, a low TEWL indicates a site with lower skin permeability. Two sample equivalence tests performed (all three rabbits) with S1D as test in reference to C ($p = 0.241$) & S1D ($p = 0.209$) were not equivalent, however S1D was equivalent to CD ($p = 0.006$). In summary, these findings suggest the involvement of calcium in the penetration-enhancing effect of Limonene, however more experiments will be needed to prove the interaction between Limonene and TRPA1 channels.

12. Conclusion and Summary

The overall aim of this dissertation was to investigate whether the mechanism of limonene skin permeation enhancing effect involved interaction with TRP calcium channels. Preliminary studies included developing and validating an RP-HPLC method for simultaneous estimation of DPH and DTZ, respectively. The first aim was to find the optimal concentration of Limonene as a penetration enhancer in DPH gel formulations. *In vitro* Franz diffusion studies were performed on DPH gels prepared in-house with three different concentrations of R-L and S-L. The two formulations, one of each R-L and S-L with the best permeation profiles across porcine ear skin were then prepared with CCB to study the next aim. In-vitro permeation studies of DPH gels, with and without CCB were performed to investigate whether DTZ blocked the permeation enhancing capabilities of R-L or S-L. These gels were further studied *in vivo* in rabbits using Dermal microdialysis technique. The dermis concentration-time profile of the gel with R-L or S-L were compared with gel containing CCB DTZ.

The preliminary study's results demonstrate that there were no physical interactions in the gel formulations between DPH and DTZ, as well as between DPH, R-L, S-L and DTZ at the *in vitro* level. The formulations R1 and S1 showing highest permeability across porcine ear skin were selected to be formulated with CCB DTZ and tested for *in vitro* permeability. Ex-vivo studies suggest that addition of DTZ to the gel might actually inhibit limonene-induced penetration enhancing effect on DPH.

In vitro MD for DPH showed that diffusion was found to be direction independent. In vivo studies demonstrated higher penetration of DPH across the rabbit skin for gel formulations containing R-L/S-L, whereas formulation with DTZ showed slightly less penetration of DPH across the skin. This may support our hypothesis that Limonene interacts with Calcium at the cutaneous level to increase the penetration of the drug, however more in-vivo experiments are necessary to further prove the hypothesis.

This study also shows us comparative results for the two enantiomers of the penetration enhancer Limonene. The results showed that the total dermal exposure for R1 was higher than S1 for an average of six probes across three rabbits. This difference in the permeation of drug can be due to difference in the interaction between two chiral molecules – Limonene and DTZ. Effect of R-L and S-L in semisolid vehicles have been studied by Monti, D. *et al* where he found R-L to be more active than S-L for Dapiprazole base [53]. He also noted that while lag time for S-L was 2.55 times that of R-L, disordering and extracting lipids was stronger than R-L. Previously, studies by Monti, D. discovered that the mechanism of monoterpenes neither involved partition coefficient nor thermodynamic activity being altered by terpenes. He suggested that possible mechanism of permeation enhancement by terpenes was modification of skin barrier properties. Further studies can be performed: 1. By increasing the number of subjects (rabbit studies); 2. By use of TRPA1 channel antagonists and/or 3. By use of techniques for live cell imaging like confocal Raman spectroscopy that produces high resolution to observe its effect on the cutaneous penetration enhancing effect of Limonene.

13. References

- [1] N. K. Jain, Controlled and Novel Drug Delivery 1st edition, New Delhi: CBS Publisher and Distributors, 2001, pp. 100 - 129.
- [2] N. Lima, D. De Sousa, F. Pimenta, M. Alves, F. De Souza, R. Macedo, R. Cardoso, L. De Moraes, M. Melo Diniz and R. De Almeida, "Anxiolytic-like activity and GC-MS analysis of (R)-(+)-limonene fragrance, a natural compound found in foods and plants," *Pharmacology, biochemistry, and behavior*, pp. 450 - 454, 2013.
- [3] I. Diez, C. Peraire, R. Obach and J. Domenech, "Influence of d-limonene on the transdermal penetration of felodipine," *Europeon Journal of Drug Metabolism and Pharmacokinetics*, pp. 7 - 12, 1998.
- [4] A. Williams and B. Barry, "Penetration enhancers," *Advanced Drug Delivery Reviews.*, pp. 603 - 618, 2004.
- [5] Y. Lan, J. Wang, Y. Liu, Q. Ru, Y. Wang, J. Yu and Q. Wu, "Effect of terpene penetration enhancer and its mechanisms on membrane fluidity and potential of HaCaT keratinocytes," *China Journal of Chinese materia medica*, pp. 643 - 648, 2015.
- [6] T. Kaimato, Y. Hatakeyama, K. Takahashi, T. Imagawa, M. Tominaga and T. Ohta, "Involvement of transient receptor potential A1 channel in algescic and analgesic actions of the organic compound limonene," *Europeon Journal of*

Pain, pp. 1155 - 1165, 2016.

- [7] M. Bandell, G. Story, S. Hwang, V. Viswanath, S. Eid, M. Petrus, T. Earley and A. Patapoutian, "Noxious cold ion channel TRPA1 is activated by pungent compounds and bradykinin," *Neuron*, pp. 849 - 857, 2004.
- [8] S. Jordt, D. Bautista, H. Chuang, D. McKemy, P. Zygmunt, E. Högestätt, I. Meng and D. Julius, "Mustard oils and cannabinoids excite sensory nerve fibres through the TRP channel ANKTM1," *Nature*, pp. 260 - 265, 2004.
- [9] M. Z. P. Guimaraes and S.-E. Jordt, "TRPA1 : A Sensory Channel of Many Talents," in *TRP Ion Channel Function in Sensory Transduction and Cellular Signaling Cascades*, Boca Raton (FL), CRC Press/Taylor & Francis, 2007.
- [10] Y. Karashima, N. Damann, J. Prenen, K. Talavera, A. Segal, T. Voets and B. Nilius, "Bimodal action of menthol on the transient receptor channel TRPA1," *Neuroscience*, pp. 9874 - 9884, 2007.
- [11] A. Joshi, A. Joshi, H. Patel, D. Ponnoth and G. Stagni, "Cutaneous Penetration - Enhancing Effect of Menthol: Calcium involvement," *Journal of Pharmaceutical Sciences*, pp. 1923 - 1932, 2017.
- [12] F. Groeber, M. Holeiter, M. Hampel, S. Hinderer and K. Schenke-Layland, "Skin tissue engineering — In vivo and in vitro applications," *Advanced Drug Delivery Reviews*, pp. 352 - 366, 2011.
- [13] S. Zsikó, E. Csányi, A. Kovács, M. Budai-Szucs, A. Gácsi and S. Berkó, "Methods to Evaluate Skin Penetration In Vitro," *Scientia Pharmaceutica*, 2019.

- [14] J. Hadgraft, "Skin deep," *Europeon Journal of Pharmaceutics and Biopharmaceutics*, pp. 291 - 299, 2004.
- [15] "Lumen Learning," [Online]. Available: <https://courses.lumenlearning.com/wmopen-biology2/chapter/structure-and-function-of-skin/>.
- [16] H. Suh, J. Shin and Y. Kim, "Microneedle Patches for Vaccine Delivery," *Clin. Exp. Vaccine Res.*, no. 3, pp. 42-49, 2014.
- [17] G. J. Tortora and S. R. Grabowski, *Principles of Anatomy and Physiology* 7th edition, New York: Harper Collins College Publishers, 1993.
- [18] H. Tanwar and R. Sachdeva, "TRANSDERMAL DRUG DELIVERY SYSTEM: A REVIEW," *INTERNATIONAL JOURNAL OF PHARMACEUTICAL SCIENCES AND RESEARCH*, pp. 2274 - 2290, 2016.
- [19] S. Rani, K. Saroha, N. Syan and P. Mathur, "Transdermal Patches a successful tool in Transdermal Drug Delivery System: An overview," *Der Pharmacia Sinica*, pp. 17 - 29, 2011.
- [20] S. S. Sultana, P. Parveen, M. S. Rekha, K. Deepthi, C. A. Sowjanya, D. Seetha and S. S. Sultana, "Emulgel - a novel surrogate appraoch for the transdermal drug delivery system," *Indo American Journal of Pharmaceutical Research Indo American Journal of Pharm Research*, vol. 4, pp. 5250-5265, 2014.
- [21] V. P. Shah, A. Yacobi, F. Ş. Rădulescu, D. S. Miron and M. E. Lane, "A science-based approach to topical drug classification system (TCS)," *International*

Journal of Pharmaceutics, vol. 491, pp. 21 - 25, 2015.

- [22] S. M., D. V. Gowda, V. N. Gupta and A. R. Akhila, " An overview on topical drug delivery system," *International Journal of Research in Pharmaceutical Sciences*, vol. 11, no. 1, pp. 368 - 385, 2020.
- [23] D. Bhowmik, H. Gopinath, B. P. Kumar, S. Duraivel and K. P. S. Kumar, "Recent Advances In Novel Topical Drug Delivery System," *The Pharma Innovation Journal*, vol. 1, pp. 12 - 31, 2012.
- [24] N. K. Jain, *Pharmaceutical Product Development*, New Delhi: CBS Publisher and Distributers, 2002, pp. 221 - 228.
- [25] R. Mehta, "Topical and Transdermal Drug Delivery: What a Pharmacist Needs to Know," in *Accreditation Council for Pharmacy Education*, Arizona, 2004.
- [26] K. Ramteke, S. Dhole and S. Patil, "Transdermal Drug Delivery System: A review," *Journal of Advanced Scientific Research*, pp. 22 - 35, 2012.
- [27] J. Li, W. Xu, Y. Liang and H. Wang, "The application of skin metabolomics in the context of transdermal drug delivery," *Pharmacological Reports*, pp. 252 - 259, 2017.
- [28] E. H. Mojumdar, Q. D. Pham, D. Topgaard and E. Sparr, "Skin hydration: interplay between molecular dynamics, structure, and water uptake in the stratum corneum," *Scientific Reports*, pp. 1 - 13, 2017.
- [29] A. Das and A. B. Ahmed, "Natural Permeation Enhancer for transdermal drug delivery system and permeation evaluation: A review," *Asian Journal of*

Pharmaceutical and Clinical Research, pp. 5 - 9, 2017.

- [30] R. Holmgaard and J. Nielsen, Dermal absorption of pesticides: evaluation of variability and prevention, Denmark: The Danish Environmental Protection Agency, 2009.
- [31] A. Hafeez, D. U. Jain, J. Singh, A. Maurya and L. Rana, "Recent Advances in transdermal drug delivery system: An overview," *Journal of Scientific and Innovative Research*, pp. 733 - 744, 2013.
- [32] N. Roy, M. Agrawal, S. Chaudhary, V. Tirkey, A. Dhway and N. Mishra, "PERMEATION ENHANCERS: A MAJOR BREAKTHROUGH IN DRUG DELIVERY TECHNOLOGY," *International Journal of Pharmaceutical Sciences and Research*, pp. 1001 - 1011, 2017.
- [33] K. Dua, V. Sharma, U. S. Sara and D. Agarwal, "Penetration enhancer for Transdermal drug delivery system; A tale of the under-skin travelers," *Advances in natural and applied sciences*, pp. 95 - 101, 2009.
- [34] M. Bharkatiya and R. Nema, "Skin penetration enhancement techniques," *Journal of Young Pharmacists*, pp. 110 - 115, 2009.
- [35] K. B. Ita, "Chemical Penetration Enhancers for Transdermal Drug Delivery - Success and Challenges," *Current Drug Delivery*, pp. 645 - 651, 2015.
- [36] S. Saini, S. B. Chauhan and S. Agrawal, "Recent development in Penetration Enhancers and Techniques in Transdermal Drug Delivery System," *Journal of Advanced Pharmacy Education & Research* , pp. 31 - 40, 2014.

- [37] B. Sapra, S. Jain and A. K. Tiwary, "Percutaneous permeation enhancement by terpenes: mechanistic view," *The AAPS Journal*, pp. 120 - 132, 2008.
- [38] P. A. Cornwell and B. W. Barry, "Sesquiterpene components of volatile oils as Ski penetration enhancers for the hydrophilic permeant 5-Fluorouracil," *The Journal of Pharmacy and Pharmacology*, pp. 261 - 269, 1994.
- [39] T. Phaechamud, S. Tuntarawongsa and P. Charoensuksai, "Evaporation Behavior and Characterization of Eutectic Solvent and Ibuprofen Eutectic Solution," *AAPS PharmSciTech*, vol. 17, no. 5, pp. 1213 - 1220, 2016.
- [40] Park, Hyo, Lee, Ji, J. & Jun and Sung-Joon, "Limonene, a natural cyclic terpene, is an agonistic ligand for adenosine A2A receptors," *Biochemical and biophysical research communications*, pp. 345 - 348, 2011.
- [41] P. M. Burnham, "Limonene - Molecule of the Month," Figshare, Journal Contribution, 2017.
- [42] W. Zhou, S. He, Y. Yang, D. Jian, X. Chen and J. Ding, "Formulation, characterization, and clinical evaluation of propranolol hydrochloride gel for transdermal treatment of superficial infantile hemangioma.," *Drug Development and Industrial Pharmacy*, pp. 1109 - 1119, 2015.
- [43] J. A. D. F. G. C.-F. H. M.-G. Joaquín Isac-García, "Basic Operation Experiments," in *Experimental Organic Chemistry*, Academic Press, 2016, pp. 207-238.
- [44] K. C. G. A. S. S. H. M. S. P. C. Z. W. J. Wishart DS, "Drugbank: a

- comprehensive resource for in silico drug discovery and exploration.," *Nucleic Acids Res.* , 2006.
- [45] A. Verma, S. Singh, R. Kaur and U. K. Jain, "Topical Gels as Drug Delivery Systems: A Review," *International Journal of Pharmaceutical Sciences Review and Research*, pp. 374 - 382, 2013.
- [46] R. Holmgaard, J. B. Nielsen and E. Benfeldt, "Microdialysis sampling for investigations of bioavailability and bioequivalence of topically administered drugs: current state and future perspectives," *Skin Pharmacology and Physiology*, pp. 225 - 243, 2010.
- [47] T. Seki, A. Wang, D. Yuan, Y. Saso, O. Hosoya, S. Chono and K. Morimoto, "Excised porcine skin experimental systems to validate quantitative microdialysis methods for determination of drugs in skin after topical application," *Journal of Control Release*, pp. 181 - 189, 2004.
- [48] E. Schnetz and M. Fartasch, "Microdialysis for the evaluation of penetration through the human skin barrier — a promising tool for future research?," *European Journal of Pharmaceutical Sciences*, vol. 12, no. 3, pp. 165-174, 2001.
- [49] "Bioanalytical Method Validation - Guidance for Industry," Center for Drug Evaluation and Research, Food and Drug Administration, May 2018.
- [50] I. PermGear. [Online]. Available: <https://permegear.com/franz-flow-cell/>.
- [51] N. Takahashi, D. Kozai and Y. Mori, "TRP channels: sensors and transducers of gasotransmitter signals," *Frontiers in physiology*, vol. 3, no. 1664-042X, 2012.

- [52] J. L. R. L. E. B. Chinmay Shukla, "Regulatory Aspects of Microdialysis: A United States Food and Drug Administration Perspective".
- [53] D. Monti, "Enhancement of transdermal penetration of dapiprazole through hairless mouse skin," *J. Control. Release*, vol. 33, pp. 71-77, 1995.
- [54] B. P. J. and .. O. G. Nilius, "Irritating channels: the case of TRPA1," *The Journal of physiology*, vol. 589, no. 7, pp. 1543-1549, 2011.
- [55] L. D. Petrocellis, V. Vellani, A. Schiano-Moriello, P. Marini, P. C. Magherini, P. Orlando and V. D. Marzo, "Plant-Derived Cannabinoids Modulate the Activity of Transient Receptor Potential Channels of Ankyrin Type-1 and Melastatin Type-8," *Journal of Pharmacology and Experimental Therapeutics*, vol. 325, no. 3, pp. 1007-1015, 2008.